POLITECNICO DI TORINO

Department of Electronics and Telecommunications

Master Degree in Communications and computer network engineering

Master Degree Thesis

Latency research of 5G on optical network

Supervisor: Prof. CURRI VITTORIO

Co-supervisor: Mr. FERRARI ALESSIO

Candidate: ZHANG WEIQI (229652)

DECEMBER 2019

Catalogy

Chapter 1 Introduction

The fifth generation(5G) wireless technology can offer plenty of benefits for example, high bandwidth, low latency, faster internet access, and large mobile coverage compared with former technics. However, in order to meet the above needs to support a given application in mobile terminal, we should deal with the key problems in 5G such as latency. In this thesis, we exploit different technologies to improve latency issues. Firstly, in chapter 2, we review the transport evolution for the radio access networks (RAN). In chapter 3, we talk about V-CRAN which is a solution to reduce latency and can increase the system throughput and the efficiency of resource usage. In chapter 4, we present a backhaul architecture for 5G based on a special device called quasi-passive reconfigurable (QPAR) to reduce the average latency, in the meanwhile, we guarantee QoS. In chapter 5, we discuss how digital signal processing (DSP) is used to support 5G to have low latency and high bandwidth efficiency. In chapter 6, we present a low-latency, high speed passive optical network (PON) by using a technology named time controlled-tactile optical access (TIC-TOC).

Chapter 2 Radio Access Networks

As the 5G technologies rapidly improving, wireless industry is facing a large change. In the past few years, the first 5G New Radio (NR) standard has released, but it only lasted less than one year then being adopted. The capabilities and applications of 5G have always been the central issue. Although many of the applications remain in conceptual form, some practical solutions are planning to take early trials by global equipment providers.

Mobile communication with low-latency and high reliability has attracted strong interest in the industrial domain, such as Internet of Things (IoT), where better latency and reliability must be guaranteed than those in traditional consumer IoT. Remote controlling applications for workers, mobile robots or autonomous vehicles are just a few examples.

The strict requirements for the above applications are requiring new solutions of the 5G radio, and communication network's transport segment as well.

Radio Access Network is always been a part of the mobile communication from 1G through 5G which provides connection between remote device and its core network (CN).

Now let's review some of the evolvement of RAN.

2.1 Extensible RAN/Open RAN

History: The extensible RAN (xRAN) Forum was founded in October 2016. It aimed on providing an alternative to the traditional closed hardware-based RAN architectures. It included vendors and operators. Developing an interoperable fronthaul interface that could be multi-vendor supported was the main task for the fronthaul work group.

Then in February of 2018, the xRAN Forum decided to combined with the centralized/cloud radio access network (C-RAN) Alliance in order to drive the RAN into a new level that led by carrier. And finally, in July 2018, the more mature version of the interoperable fronthaul specification was published.

The following we have the details of the specification:

- efficient bandwidth scaling as a function of user throughput and spatial layers to address increasing bandwidth needs and massive MIMO deployments;
- support for LTE and NR, with different RU product configurations, including massive MIMO beamforming antenna systems;
- advanced receivers and coordination functions;
- Ethernet-based transport layer solutions;
- extensible data models for management functions to simplify integration.

2.2 Disaggregated RAN

The identification of the functional modules in the RAN and the specification of the interconnect interfaces make it possible to choose a wide range of deployment options. The various functional entities radio unit (RU), distributed unit (DU), centralized unit (CU)-user plane (UP) and CU-control plane (CP) can be placed in different physical locations according to operator requirements, physical site restrictions, transport network topology, delay and capacity constraints, and computing resource availability or specialization.

Figure 1 shows a selection of example functional placement options based on the assumption that the RAN may have the following functions:

- cell site,
- aggregation site [intermediate site which is used for transport aggregation, and may be used to host legacy baseband unit (BBU) hoteling],
- edge site (most centralized site in RAN).

As shown in the figure, the leftmost part corresponds to the C-RAN where all processing functions are in the same location, except for the RUs which are the cell sites. Then, on the rightmost part of the figure that corresponds to the normal deployment mode in which all function elements locate in the radio site. In the dual split RAN part, we combine the services which are not highly latency sensitive with the latency-sensitive services on the cell site.

Except for the above flexible placement, dynamic placement can transfer the failed processing elements to make sure the load is still in balance.

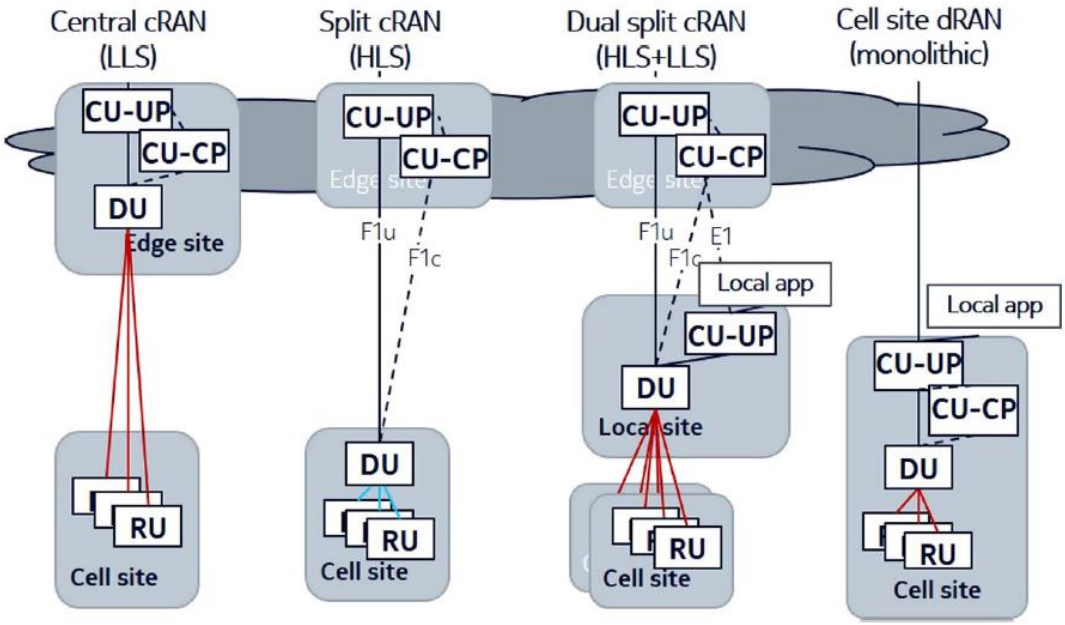

Fig. 1. Disaggregated RAN, selected functions placement options.[1]

2.3 C-RAN

Centralized/Cloud-radio access network(C-RAN) is a foreseeable architecture for mitigating the above problems in 5G networks. In C-RAN, a cell site (CS) device is functionally divided into two elements, the centrally located Base-Band Unit (BBU) controls the radio signals of hundreds or even thousands of remote radio heads (RRHs) connected through the preamble network. While implementing C-RAN architecture has many advantages, it is also very challenging. Particularly in designing a low cost and high efficiency network in the meanwhile satisfying the delay and capacity reequipments. The optical network is obviously the best choice for the 5G fronthaul due to its features such as low latency, high capacity and scalability. As a result, it needs to be strategically designed.

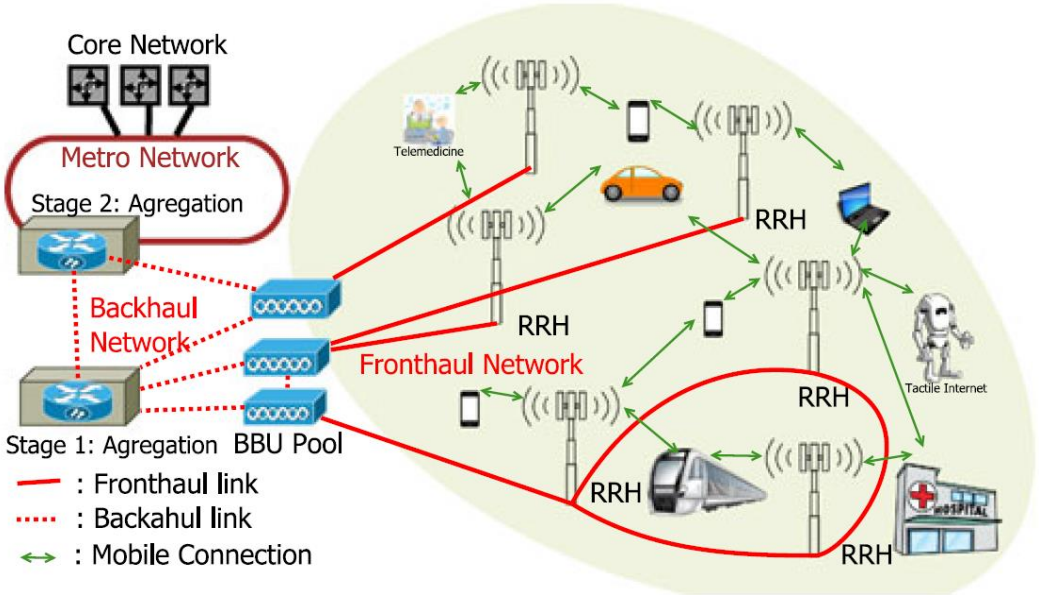

Fig. 2. Centralized radio access network (C-RAN).[1]

Figure 2 shows the architecture of 5G C-RAN and its transport network.

We can see that those RRHs or wireless cells that are near the end users are connected with the BBU pool using fronthaul network while BBU pools which are deployed in different locations are connected with the next aggregation node through the backhaul network.

In the next chapter, we will discuss about virtualized-CRAN which is on the basis of the optical network (PON) architecture that can reduce latency.

Chapter 3 virtualized-CRAN

3.1 System Architecture

3.1.1 Architecture Overview for V-CRAN

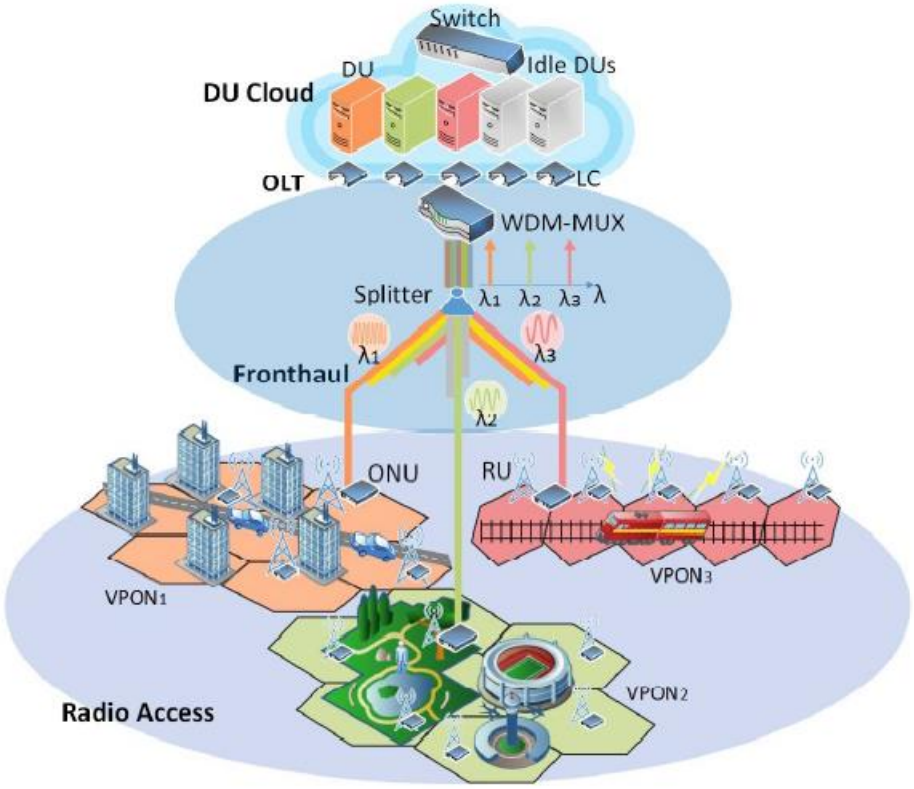

Fig. 3 V-CRAN architecture overview.[4]

As shown in Figure 3, in digital unit (DU) cloud, DUs are implemented through commercial servers that provide real-time baseband processing. DUs connect with a high-speed Layer-2 switch, which gives supports to the switch between signaling and data in DUs. In order to satisfy the strict latency requirements of fronthaul segment, Time-Wavelength Division Multiplexing Passive Optical Network (TWDM-PON) is used. Also, it can provide other requirements such as enough bandwidth, low cost and low

energy consumption [42]. TWDM-PON has tree topology with multi-stage, it has an optical line terminal (OLT) as its root node, and some passive splitters as intermediate nodes. As for leaf nodes, it uses optical network units (ONUs). OLT locates together with DU cloud, they use optical transceiver and linecard (LC) to connect their supported wavelengths and DUs. The LC is coupled to a WDM multiplexer/demultiplexer (MUX) that aggregates traffic on a plurality of discrete wavelengths. DU cloud farther from the passive splitter can split fibers, and increase the coverage of TWDM-PON. Each ONU is equipped with a tunable transceiver that uses the radio unit (RU) as a terminal for the fronthaul optical network. Resource blocks (RBs) are allocated in its spectrum band to serve the covered area by a RU.

3.1.2 Virtualized PON in V-CRAN

From figure 4, we can see that a VPON is an optical channel which pass in the wavelength between a set of ONUs and an LC. RU summarizes the traffic to a VPON then transmit to the DU. In this manner, the RU will be associated with the same DU. Within each VPON, V-CRAN can enlarge the RAN coverage and throughput by implementing Joint Transmission (JT). By using JT, multiple neighboring Rus can be adjusted to transmit common signals to a UE on the same RB. As a result, we can get useful information by converting the interference. In order to achieve good performance, JT needs heavy processing resources, extremely low latency (1ms or even less) and global information about he radio resources of plurality of cells. Before we make the schedule decisions, we need to copy the data and signaling information and transmit to all coordination RUs [40].

The reasons why VCRAN can decrease the latency for JT will be explained as followed:

a) VPONs can provide adequate bandwidth for transmitting the data among Rus and DU.

b) Specialized software and hardware are equipped to DU, so that JT controller can use it to provide signaling and data for RUs.

c) VPON directly connects the DU to the LC so that load allocation in DUs can be handled in optical layer fast on a per-cell basis rather than using

a complex Layer-2 switch on a per-frame basis. For example, if traffic load from a cell tends to be stable in e.g., minutes, aggregating or balancing the load should be done on a per-cell basis in layer 1 rather than done on a per-frame basis in layer 2. This operation is done in the optical domain on the fronthaul by V-CRAN which can reduce the complexity of DU cloud and also latency, considering CoMP's strict latency requirement (typically 1 ms or even less).

We can increase the throughput for UEs by using JT after we form the VPON. By doing so, we can separate the radio access area into several service areas, every service area is connected to a VPON which is shown in figure 3. For example, we can form a VPON1 along the railroad track to serve the trains. Also, we can form a VPON2 to cover hotspots in airports, shopping malls and schools.

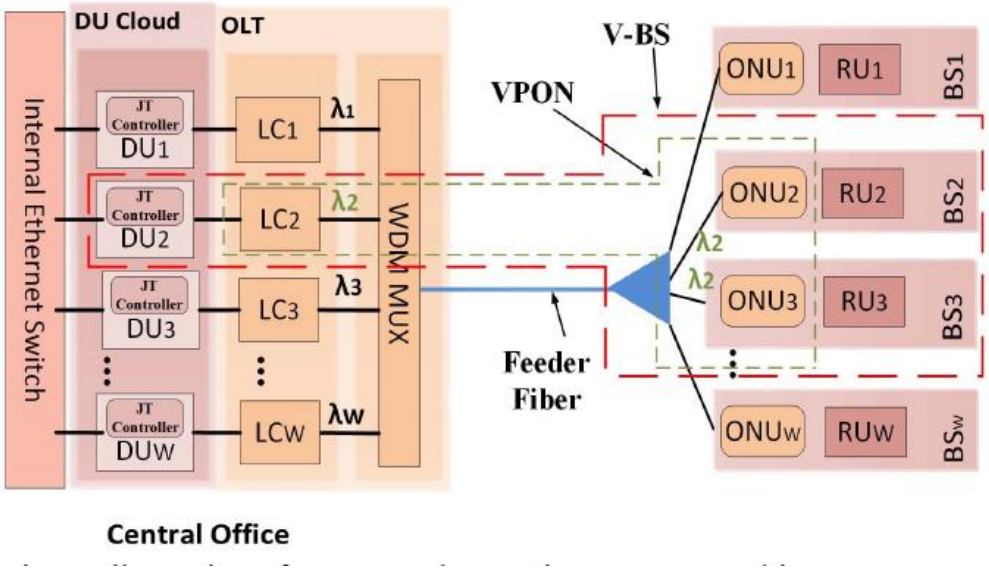

Figure 4. Illustration of VPON and V-BS in V-CRAN architecture.[4]

3.1.3 Virtualized Base Station (VBS) in V-CRAN

In V-CRAN, we form a VBS which is user-centric for each UE to enlarge the throughput. We can form the VBS for a UE shown in Figure 4 by the following steps:

a) We need to assign virtualized baseband processing resources in shared DU, in order to provide JT service.
b) We assign bandwidth resource in shared VPON, in order to transmit data and signaling from DU to the radio sites.
c) We choose a group of RUs (JT group) coordinated by the same DU to transmit the signals to the UE together.

In V-CRAN, we can strengthen the useful signal by forming VBS dynamically around the UE. And we cancel the inter-cell interference (ICI) by assigning non-overlapping RBs to VBS of other UEs. In order to implement JT, we should select a group of RUs which is adjacent to the VBS to provide good signals. There are 2 constraints which must be satisfied for selecting RUs:

a) The selected RUs must be associated with the same DU by a VPON. It means that we must adjust their wavelength of their optical transceivers into the same value, which is also called wavelength-uniformity constraint.
b) The selected RUs must transmit data to a UE through the same RB, which named resource-block-continuity constraint.

3.1.4 Reference Architectures for distributed RAN (DRAN) and CRAN

We compare our approach with DRAN and traditional CRAN. In traditional CRAN, although DUs locate in the DU, but there's no sharing of DUs and wavelength between cells, so dedicate optical transceiver and an active DU is needed to serve the cell. While in DRAN, DU locate with its RU at the cell site. DU is active all the time and it's not sharable to other RUs. Also, DU does not need to coordinate the inter-cell and fronthaul network is not needed.

3.2 ILLUSTRATIVE NUMERICAL RESULTS

In this section, we will demonstrate why V-CARN has better performance in terms of throughput and energy consumption comparing to DRAN and traditional CRAN quantitatively by a constraint programming (CP) based mathematical formulation presented by [9]. Table 1 [43] includes all the simulation parameters. The spectral bandwidth is 10MHz for every cell. RBs of a cell are grouped into g larger resource block groups (RBGs), then we equally assign them to UEs in order to have maximum one RBG for each user. We choose g=5 to reduce the variables of the CP model to get the optimum result. The number of UEs are set from 9 to 90 which are uniformly distributed according to the utilization factor (u-factor) m which is the ratio of the number of UEs to the total number of RBGs in the network. Following results are came from the computation of 200 Unrelated instance and with a 95 percent confidence interval.

Parameters	**Value**
Deployment	19 BS, ISD=1000m, hexagonal grid, wrap-around
Path loss	L=15.3+37.6log(d) (3GPP Typical Urban)
Shadow fading	std dev 8 dB
Spectral bandwidth	5~20 MHz (group into 5 RBGs)
Wavelength bandwidth	10 Gbps (maximum 5 wavelengths)
Max RU P_{TX}	20 W (4 W/RBG)
UE sensitivity	-103 dBm
Noise PSD	-174 dBm/Hz
Power consumption	P_{RU}=20 W, P_{BS} =600 W (DRAN), $P_{DU\text{-}hotel}$ =500 W, P_{DU}=100 W, P_{LC}=5 W, P_{ONU}=7.7 W

Table 1. simulation parameters.[43]

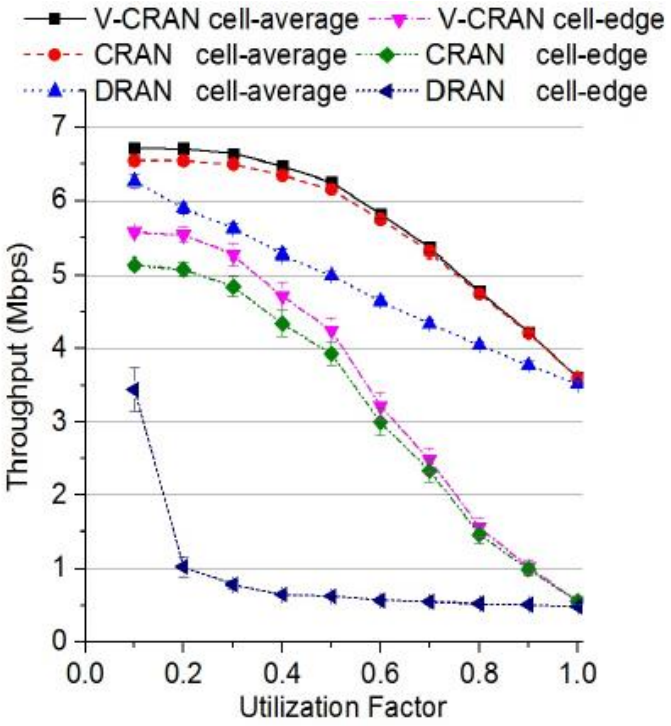

Figure 5. Average throughput (per user) for all users (cell-average) and 5% worst-case users (cell-edge) with 10 MHz bandwidth.[4]

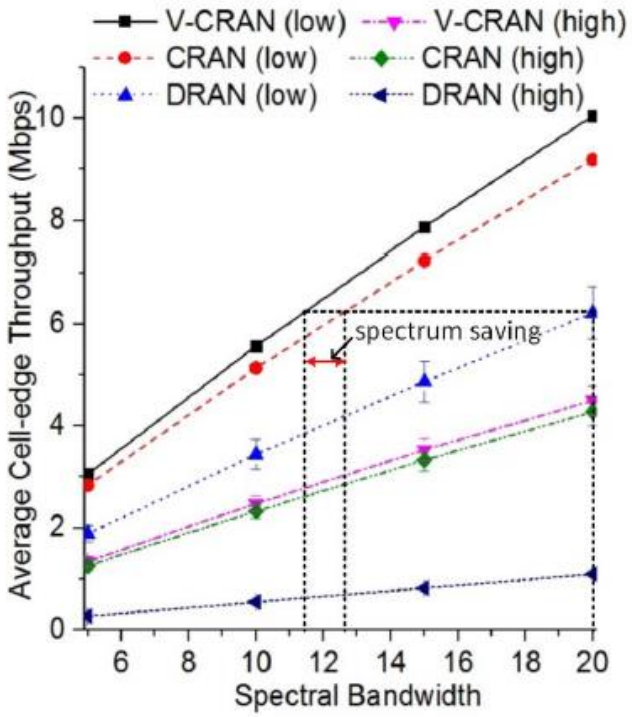

Figure 6. Cell-edge throughput at low u-factor (0.1) and high u-factor (0.7).[4]

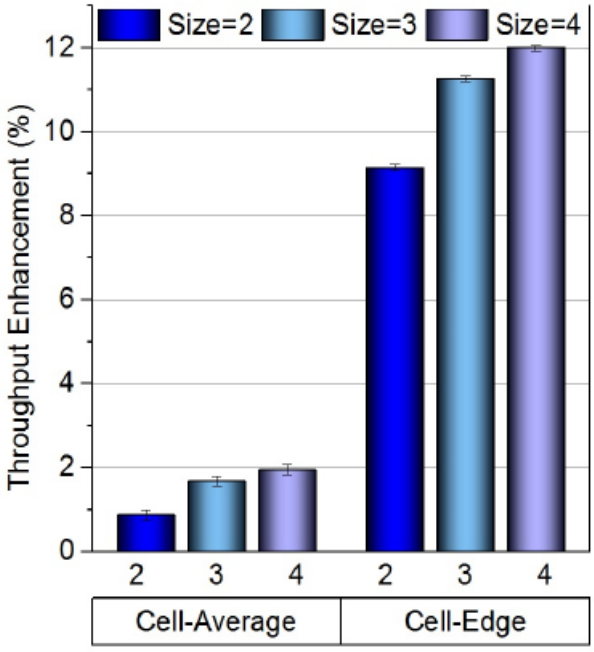

Figure 7. Percentage of UEs supported by JT service vs. load ratio for optimal VPON formation and random VPON formation with 10 MHz spectral bandwidth.[4]

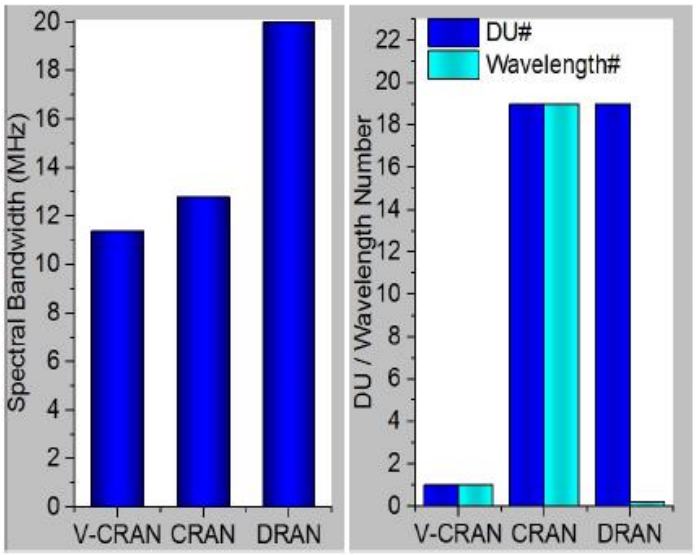

(a) Spectral bandwidth usage.

(b) DU and wavelength usage.

Figure 8. Resource usage of V-CRAN, CRAN, and DRAN at low u-factor.[4]

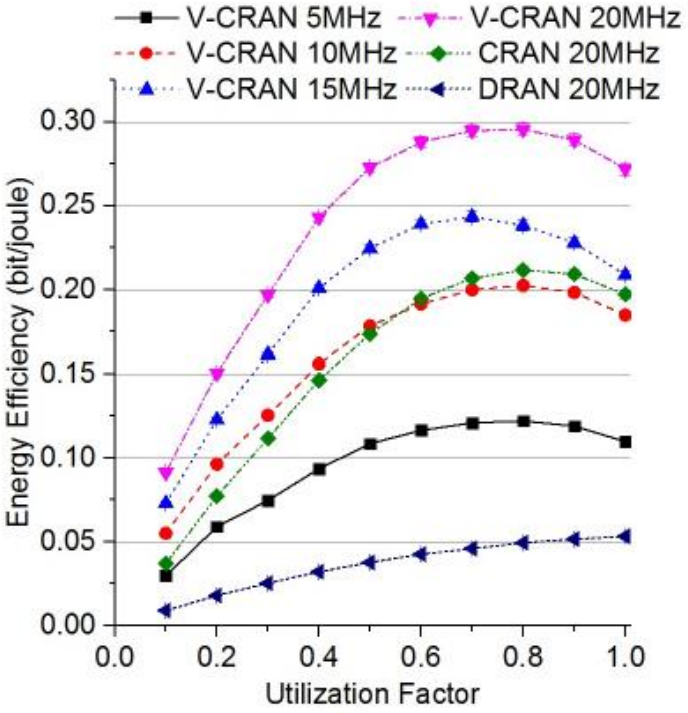

Figure 9. Energy efficiency of V-CRAN with bandwidth from 5 MHz to 20 MHz, and CRAN and DRAN with 20 MHz.[4]

Let's start from Figure 5, we plot the average throughputs for cell-average and cell-edge users by increasing the numbers of utilization factor (u-factor). Obviously, DRAN achieves the worst result of throughput. When the u-factor is increasing, there will be higher interference, resulting in rapid degradation of the throughput. For traditional CRAN, it behaves better than DRAN because ICI cancellation which is a technique of Coordinated Multi- Point (ICIC) can decrease the interference, typically for low u-factor, that when RB resources are sufficient, it's easier to avoid overlapping between RB-user assignments. By using JT, V-CRAN can further increase the throughput by 25 percent for cell-average users comparing to DRAN, meanwhile the throughput gain is more impressive for cell-edge users. Although the performance is much better, there is still

some shortage. As the value of u-factor becomes larger, the throughput gain for V-CRAN is less, which is because the VPON can support fewer cells, and thus less JT services can be provided.

In Figure 6, we do the simulation under two conditions: high and low u-factors and we set the spectral bandwidth from 5 to 20 MHz at every cell. Then we plot the cell-edge throughput of DRAN, CRAN and V-CRAN. As we told before in figure 5, V-RAN achieved the highest throughput. While in figure 6, we estimate the same throughput which DRAN can achieve with 20 MHz at load u-factor by marking (dotted lines) the bandwidth required by CRAN and V-CRAN. Comparing these three architectures, traditional CRAN can save about 7.1MHz (35.5%) while V-CRAN can save about 8.6 MHz (43%), respectively. The better performance of V-CRAN is from the JTs. Traditional CRAN and V-CRAN can save more bandwidth for high u-factor thanks to ICIC.

In Figure 7, we typically study the influence of the size of JT group to the gains of cell-edge throughput and cell-average throughput. U-factor is set to 0.1 in order to reduce the influence of ICI and focus more on JT. Due to the reason that for the cell-central UE, the adjacent cell is too far to provide useful signals compared to the host cell. Furthermore, the performance gain will saturate if we keep enlarging the size of JT group, because the additional cell is too far from the UE and its signal has only little contribution or even can be ignored.

In Figure 8, we compare the wavelength and DU usage. In this simulation, we don't consider the wavelength and switch-off of DUs in traditional CRAN and DRAN. Thus, the number of the cells is exactly the usage of DU. In DRAN, we do not have fronthaul, so the use of wavelength is zero. V-CRAN can decrease wavelength and usage of DU because of the sharing between wavelength and DUs. Also, energy consumption can be saved in V-CRAN by switching-off unused resources.

At last in Figure 9, energy efficiency (EE) is compared of the above three architecture [44] which is the number of bits that can be sent by consuming one Joule (for example total energy consumption/total throughput). Obviously, we can see from the figure, V-CRAN gets more EE than DRAN and traditional CRAN because V-CRAN can decrease power consumption and increase the throughput. Notice that compared with 20 MHz of traditional CRAN, V-CRAN of 10 MHz has similar EE. Also in the range of 0.7~0.8 of u-factor, we find that EE reaches the max, that's because ICI limits the system throughput for high loads, thus limits EE.

Chapter 4 Quasi-passive and reconfigurable

4.1 Background

First, let's briefly introduce Quasi-passive and reconfigurable (QPAR) principles, functions and implementations.

As shown in Figure 10, this is the functionality of a QPAR node.

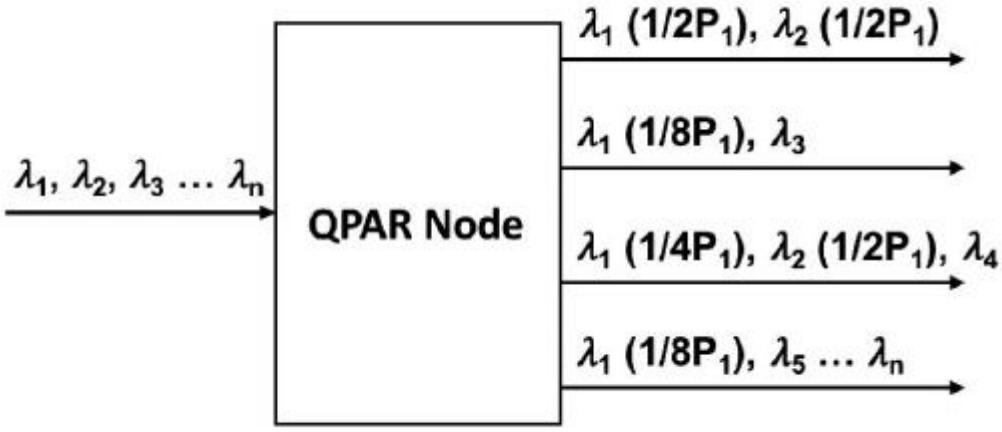

Figure 10. QPAR device functionality: sample configuration.[10]

The propagated signal through the QPAR node is a WDM(wavelength division multiplexing) signal which has N_λ wavelengths. We can see from the figure that broadcast, unicast and multicast functions are available at the same time. Noticed that, the QPAR device can multicast to a subset of output ports with no loss and different power slitting ratios. There is no power loss and blocked, because the power is reassigned which is different from the traditional wavelength selective switches [47].

Generally speaking, there are four dimensions of a QPAR node:

$N_{in}\times N_{\lambda}\times N_{p}\times N_{out}$, that is the number of input ports, number of wavelengths, number of possible output power levels and number of output ports in order. The most important device in QPAR is optical latching switch (OLS) [45], which can usually be implemented using microelectromechanical systems (MEMS) or magneto-optical effects. In our topic we use MEMS-based OLS because they consume less power. Also, QPAR node can be used for bidirectional signal transmission by providing extra components for example circulators or optical band filters. But in this chapter, we do not detail it.

4.2 QPAR in 5G backhaul networks

As discussed before, there are many requirements for 5G backhaul networks, such as flexibility, being reliable and dynamic and able to support bit rates larger than 100 Gbps. In this part, we will particularly discuss about the advantages for 5G networks using QPAR and we will present a simulation to compare the latency of fixed networks with multicast and unicast networks. The multicast network can be presented by using a QPAR, or a multicast wavelength selective switch (WSS) or a passive splitter. While in the unicast network, a QPAR without power consumption, or a unicast WSS or a passive splitter can be presented. At last, we will also discuss the advantages of flexible power allocation when using QPAR which compared to a multicast WSS or a colorless passive splitter. A new node named Pseudo-Passive Reconfigurable Node (PPAR) which is all-active (pseudo-passive) and low power consumed is also analyzed and compared as a replacement of QPAR but not detailly.

4.2.1 Proposed 5G network architectures

Let's take a look on Figure 11. It's a mesh topology that use multi-input ports QPAR (MI-QPAR). Wavelength in this topology can be routed from any base station (BS) to other BS or multiple BS by using the QPARs because it can allocate flexibly allocate the power, thus it can form point-to-point or point-to-multipoint connections at the physical layer between BSs. Usually, the connection is with an adjacent BS, so it's a single hop, while in multi hop cases, the blocking probability would increase because of the constraint of wavelength continuity. We can use a centralized control algorithm because the QPAR node can be reconfigured remotely and powered. Another advantage of using a mesh topology is that we can use a large number of redundant paths to recover the traffic.

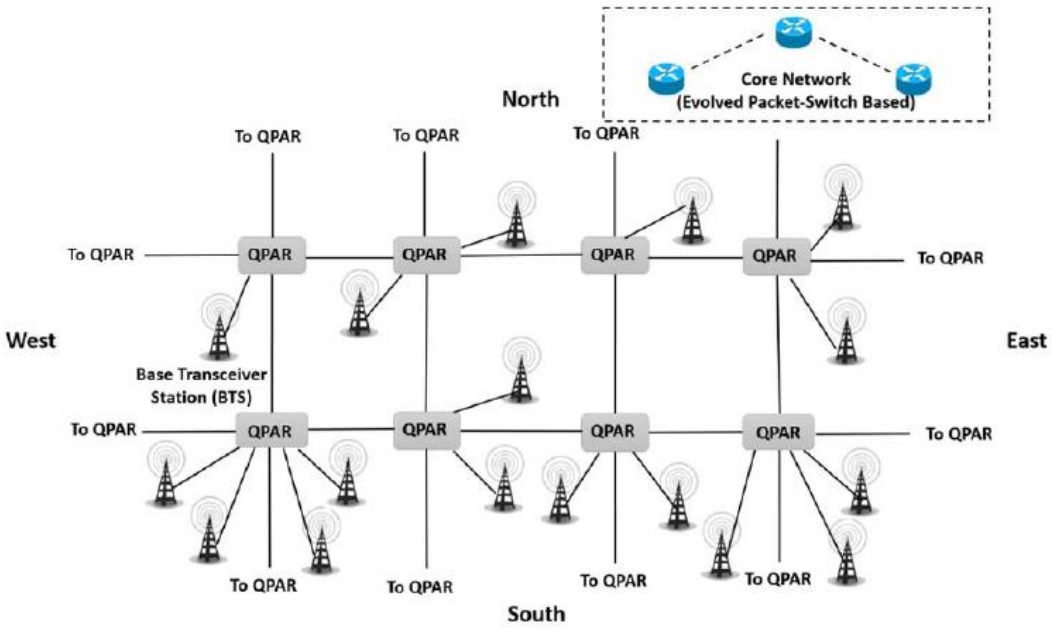

Figure 11. 5G mesh network with QPAR.[10]

Although mesh topology has many benefits, but to deploy such a

topology is very expensive in practice. Figure 12 is an alternative which is a hierarchical network. The capacity of the QPAR nodes increase while it's more closing to the core. There must be at least two unrelated paths to protect fault to the core of all QPAR nodes. If we decide to use this type of network, the PON architecture that is not protected, is the base of the edge. This PON architecture has single input QPAR which is connected to multiple BSs through a passive splitter in a single port. This hierarchical network is better for distributing and aggregating the traffic. Because most of the backhaul traffic will eventually reach the core. However, the latency my be affected due to the fact that the traffic has to go up to the next layer then go back down.

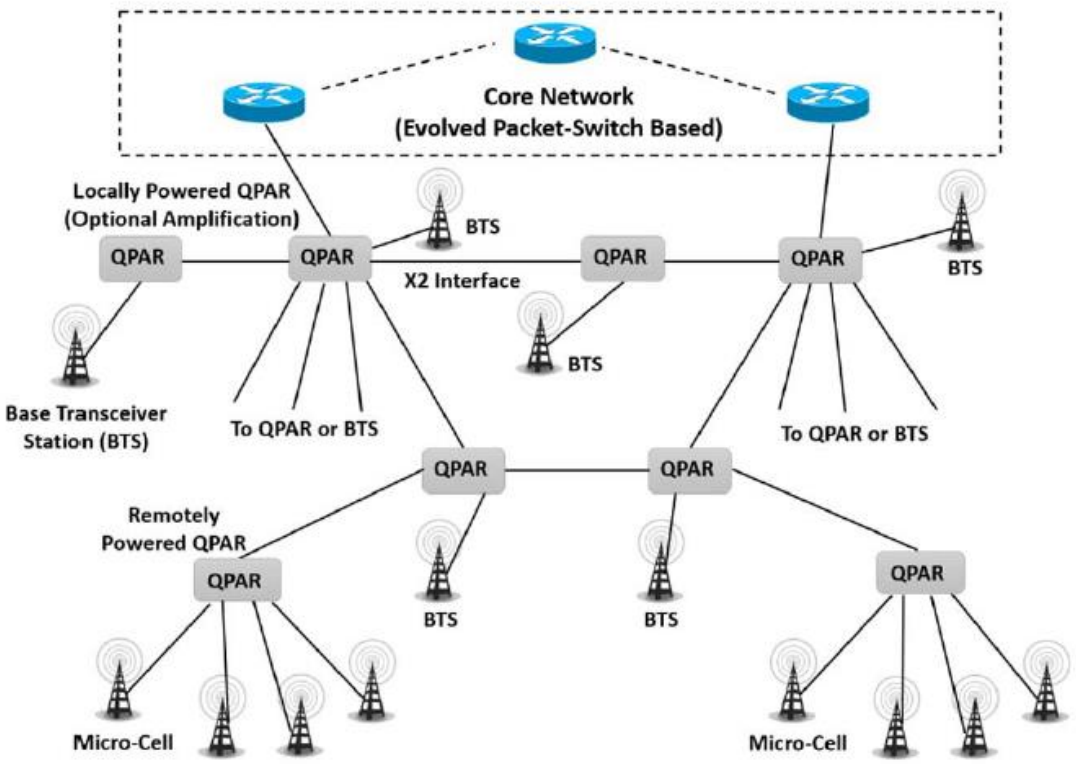

Figure 12. 5G hierarchical network using QPAR.[10]

It’s obvious that there is advantage of the latency if we use point to point optical circuits between BSs and the core. Thus, we should focus more on finding a cost less development of a shared PON. In this PON, we share the wavelengths by multiple BSs for backhauling packet switching. In Figure 13, we do a simple simulation of traffic engineering case for a TWDM-PON. The packets can be both backhaul or fronthaul data. It’s easier to evaluate the power and latency by using a QPAR node. We can know that TWDM-PON is a multicast network protocol, because in this network we can share a single wavelength among many ONUs which is served by the OLT.

But in the traditional network architecture which is based on the traditional passive splitter, wavelengths are broadcast to ONUs, thus the ONU needs to be an adjustable filter. In a multicast network which is using a QPAR or WSS, we should be able to assign the appropriate wavelength to the suitable ONU. And furthermore, the ONU can be a simple fixed receiver. From Figure 13, the network provides services to three different areas which are stadium, business and residential area. The optical node is used depending on the flexibility level. Let’s assumed that in terms of wavelength allocation, the supported network has three different levels of flexibility which will be described as following:

1) Fixed wavelength allocation to zones: at the starting time, we make sure the allocation of the wavelength to different zones. This case is easily

implemented by using fixed filters and a passive splitter. In the BSs, there will be fixed transceivers.

2) Reconfigurable wavelength allocation to zones: one wavelength to one zone, but it can be re-assigned. The first method to set the optical node is using a 1x3 WSS with each port connected to a passive splitter. By using this, power is shared among all the BSs in one zone. The second method is that we can use QPAR with no dynamic power assignment capability used. The easiest one is using a passive splitter.
3) Reconfigurable wavelength allocation to base stations: we allocate wavelengths to every BS, by doing so, we can assign the wavelength to a whole zone, or just part of the zone, or cross different zones. In this level of flexibility, the optical node could be a QPAR, or a multicast WSS, or a passive splitter.

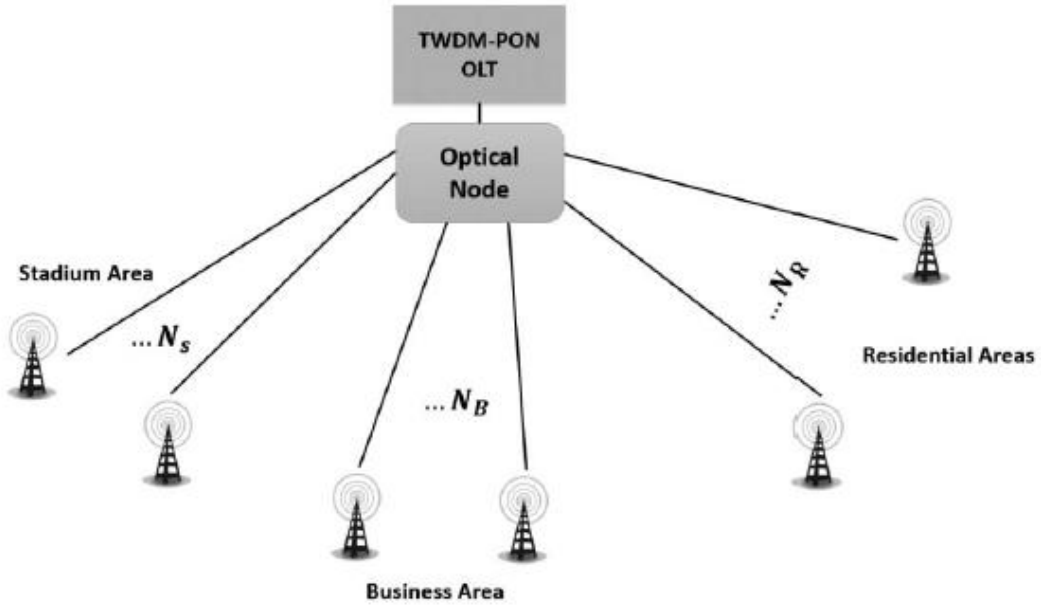

Figure 13. simulation scenario.[10]

We assume that in any cases, the BS can only transmit and receive the packet in one wavelength at one time. We should notice there is no color for passive splitter, and all wavelengths are split towards the BS. Therefore, we request there must be one adjustable transceiver in every BS in order to allocate wavelength and adjust the other wavelengths. In QPAR and WSS cases, we can route the wavelength selectively to the ports. So if we are sure that the wavelengths that we use are within their optical bandwidth, then the BSs only need to be fixed transceivers. The OLT will be reset for routing the assigned wavelength towards right ports which will also reduce the requirement for the expensive transceivers.

We do a downlink simulation of a typical TWDM-PON. Assumed that we have 64 BSs and 4 wavelengths. We divide the BSs to 24 for stadium, 24 for business and 16 for residential. To the allocation of the certain wavelength, at least one wavelength is assigned to one field by us, and we assign the 4th one to the zone with excellent service. We should guarantee at least a wavelength for a zone, for the rest ones, we allocate them to the zone which needs the highest load. Among the wavelengths, the network load will be equally assigned for reconfigurable wavelength to BSs. We assume the traffic that goes to OLT will be Poisson, then the rate of peak data has been set as less than 100gbps which uses a leaking barrel shaper. The rate of wavelength's record is set to 10 Gbps. The value of the packet is between 1000B and 1500B. The larger packet sizes are chosen because

most of the current LTE returned packs have been big, because of high video, FTP traffic as well as HTTP traffic. Suppose the traffic is 5 million requests per second, so the wavelengths are overloading averagely. Suppose there will be an infinite buffer in OLT, we calculated the average latency that the base station experiences in a 10 milliseconds transmission window. We believe that this overload situation allows for a better comparison of the three settings to improve latency. Wavelength assignment has been completed on the basis of the load within various areas, and it is assumed that the load keeps changing in various periods in a day.

Multicast WSS and QPAR reconfiguration time is in the right sequence, from several hundred microseconds towards several milliseconds. To the case of traffic engineering under consideration, the changes of load (as well as reconfigurations) are even larger (minute-hour). Therefore, the whole impact of reconfigured time to latency can be ignored. Meanwhile, the transceiver's resonating period will be approximately some microseconds, and it can be ignored when comparing with reconfigured frequency. Therefore, within this research, the time of the arrival of the pack at OLT as well as arrival of the destination are only to be taken into consideration by us.

In this research, we focus on the gain of a single node.

1) Queuing Latency: Figure 14 is to show the average packet transmit

latency in various times of a day. For example, between 9 am to 5 pm, the load's about 50 percent or 70 percent is supposed to be used for business zone. Similarly, during the evening, 50 percent or 70 percent of load is gained in the residential area, when the sports time comes, 50 percent or 70 percent of load will be supposed as coming from gym district. It can be seen that the average latency for reconfigurable wavelength assignments to BSs is very low at any time of the day due to load imbalance or medium or large. Also, we can see that, by using this scheme, the latency variance among various periods of day along with medium-large unbalanced load has been considerably smaller (latency variance in multicast network is about 2μs). This is mainly because of the maximum flexibility in distributing the load between wavelengths. The results of the simulation of the scenes in the upstream are able to represented through increasing the extra latency to the outcomes for obtaining resource access control delays.

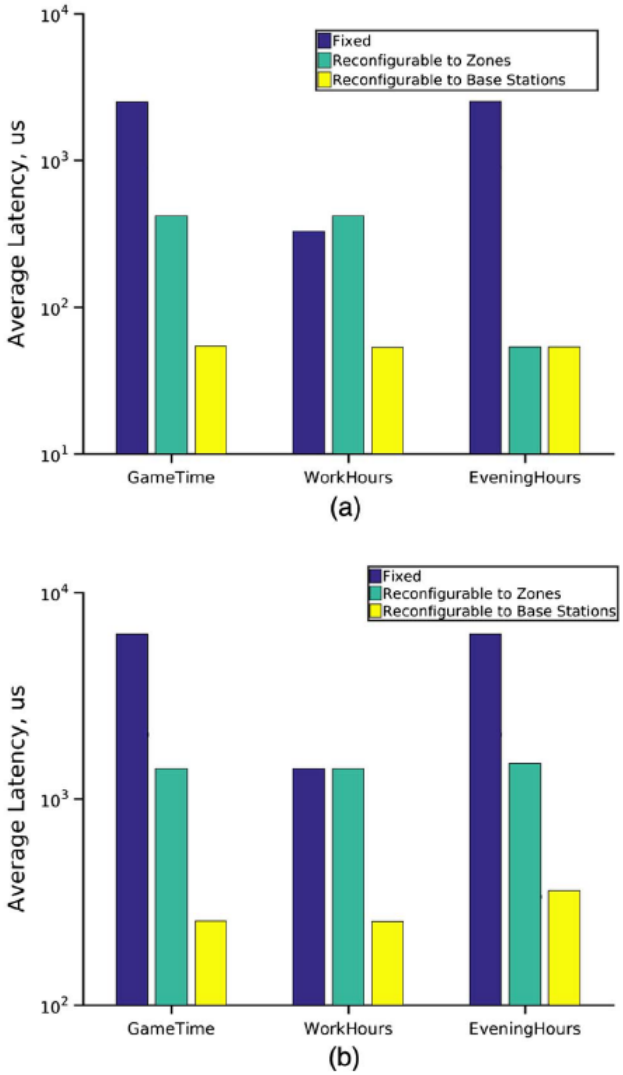

Figure 14. Average queuing latency during different times of day for the fixed, unicast, and multicast networks. (a) 50% of the load to Single zone, and (b) 70% of the load to a single zone.[10]

We also do a simulation where applications such as CoMP support inter-BS communication. In this simulation, 2 cases have been compared by us : Bi-QPAR to be an optical node (see Figure 13) , while a QPAR node with multiple input ports (MI-QPAR) to be an optical node.

As for BI-QPAR, payload need to cross OLT. Later it will be rerouted to the right BS. By using MI-QPAR, payload is routed straightly towards the right one or more BSs. The only limitation to form a point-to-multiple

point connection of the device to the frequency is the response time such as the period between the adopted electrical controlling signal changes and optical signal changes. To QPAR devices using 2 x 2 OLS, the reacting time will be hundreds of microseconds. In such cases, PPAR devices is a better solution which is more energy-efficient to support high reconfiguration frequencies.

In the simulation, we suppose that the communication data of BS is distributed uniformly, the value is between 0.1 to 1 ms and it's in the stadium zone. This time, we use point to point BS communication. Considering there is 70% of the load on downlink which goes to the stadium zone, and suppose the total downlink load is 40%. Furthermore, there's no priority to communication within base station. To the BI-QPAR scenes, supposed that communication within base station takes an Ethernet pack size form. From Fig 15, we can see he average delay of intra-BS as well as downlink pack. By adopting MI-QPAR, its value of intra-BS latency will be smaller and the average latency of the downlink packets is reduced by two orders of magnitude because inter-BS communication is not included of the downlink data.

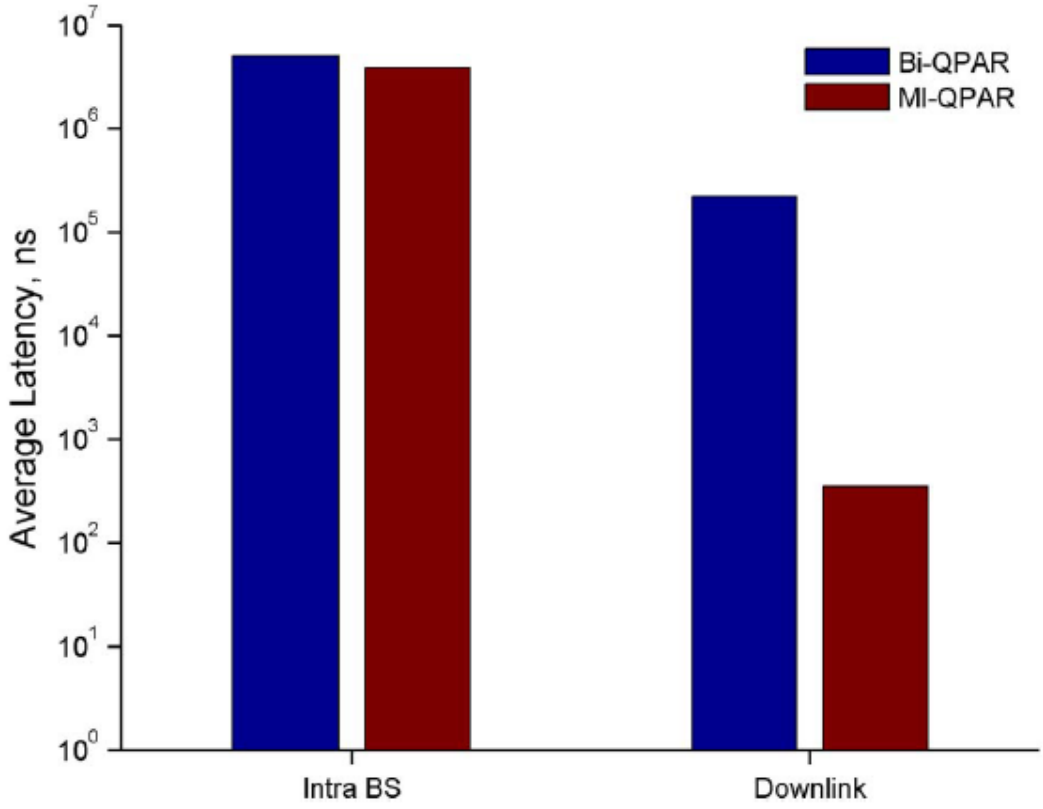

Figure 15. Assume the average queuing time of communication between BS.[10]

4.2.2 QPAR within 5G backhaul structures: advantages and disadvantages

Within optical network, a QPAR node has advantages in terms of delay that will be of great importance to 5G wireless network. It can reduce latency because flexible network allocation is available which allow for intelligent dynamic bandwidth allocation protocols. Thus, it's easier for integration of backhaul and fronthaul pack within the network of optical access. Using MIQPAR in a mesh or hierarchical topology makes it easy to set up links of point to point as well as point to multipoint for the applications with low-latency, for instance fast handoffs, CoMP, and more. Another benefit of using QPAR is that power sharing is only in the required number of ports. Since QPAR nodes can be remotely reconfigurable, all of the flexibleness is able to be achieved through the least maintenance on optical node. QPAR nodes can use the fixed transceiver of the BS instead of the adjustable transceiver to achieve reconfigurable wavelengths assignment.

Although QPAR devices are ideally beneficial, the main shortages of current discrete component designs are lack of insertion loss and scalability of the device. It's difficult achieve the advantage that the extended network can reach a large number offend users in the practical QPAR discussed before. There is a much higher inserting loss in QPAR, which is probably because of the device limitations. QPAR is on the basis of OLS and 3 dB

power splitter, while OLS adopted within the design is on the basis of MEMS with relatively large losses. In addition, coupling losses among neighboring elements cause high insertion loss in QPARs as well. With the OLS and photonic integration techniques improving, we believe the losses of QPAR insertion can be reduced. Noted that, no matter how large is the losses of device insertion, we can always have the advantages of QPAR's flexible wavelength and power distribution functions. Comparing to the reset node, being “quasi-passive” is the strength of QPAR, without requiring any power in stable situation operation. Thus, it is able to improve the energy efficiency of the network greatly.

Chapter 5 DSP for High-Speed Fiber-Wireless Convergence

In recent years, digital signal processing (DSP) has been applied to supporting common public radio interface (CPRI)-based PTP transmission for improving the efficiency of spectral, and cut down on processing latency. Passive optical network (PON) is suitable for Ethernet-based CPRI (eCPRI)-based point-to-multi-point (PTMP) transmission. Next-generation PON can provide mobile fronthaul through great efficiency, little cost, high performance, as well as low-latency by using DSP. In the following, the latest progress by making use of DSP to reaching mobile fronthaul with higher performance as well as lower latency through CPRI also eCPRI.

5.1 DSP for PTP CPRI

CPRI transmits digital wireless signal waveform within IQ data, no matter what real flow (or RB application) will be during the provided time. Therefore, comparing with eCPRI, it has less inefficiency of bandwidth. For improving CPRI's bandwidth effectiveness we need to use compression technology [49].

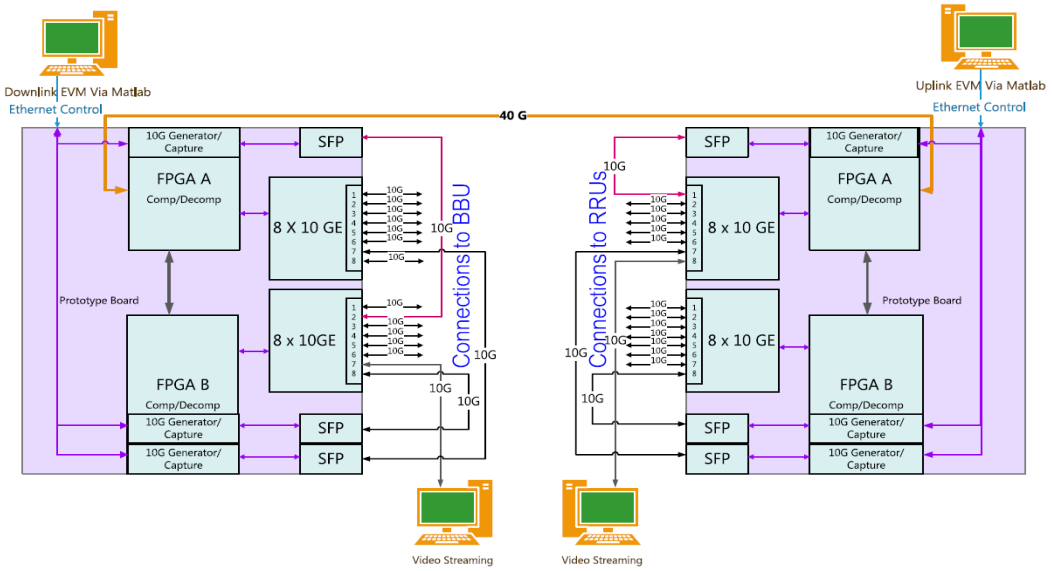

Figure 16. Diagrammatic sketch in the actual-time CPRI-on-Ethernet system with sixteen 10GE dual-direction links, 2 transceiver plates, every with 2 Xilinx Virtex-7 FPGAs, as well as 2 10-kilometer fiber spools to dual-direction transferring.[50]

Figure 16 indicates the diagrammatic sketch in the actual-time CPRI-on-Ethernet system. Within the system, the actual-time process of optical transferring in off-line wireless signal based on CPRI has been taken into consideration by us. It can simulate RAN. On the sender end, sixteen CPRI-bearing 10GE inputting to provide CPRI information. Every title of CPRI includes data, for instance an index of wire, an index of carriers, a transmission time interval (TTI) pattern, and a pack pattern. Figure 17(a)

indicates a diagrammatic sketch for a DSP-transmitter. Its total throughput of CPRI is one hundred and twenty Gb/s. When decoding for 10GE MAC, 8B/10B is performed together with that the IQ bit is taken away from Control Word (CW) bit. When the CW bit is transferred with no contraction, IQ bit is contracted with the contraction filters, and then block standardization together with quantification are performed. Contraction filters are the 4:3 decimation filters. Block standardization has been applied to reducing dynamic scope within inputting signals. When contraction has been done, the entire rate of data is approximately forty Gb/s, then the transceiver modules of forty Gb/s Quad Small Form Factor Pluggable (QSFP) is used to transfer information over the ten kilometers SSMF connection by us. To receiver, FPGA plate receives forty Gb/s signals as well as performing a DSP reconstruction for rebuilding primitive 10GE signal along with the CPRI. DSP is adopted for the received procedure as stated within Figure 17(b). Efficiently, DSP receiver performs opposite procedure of DSP transmitter.

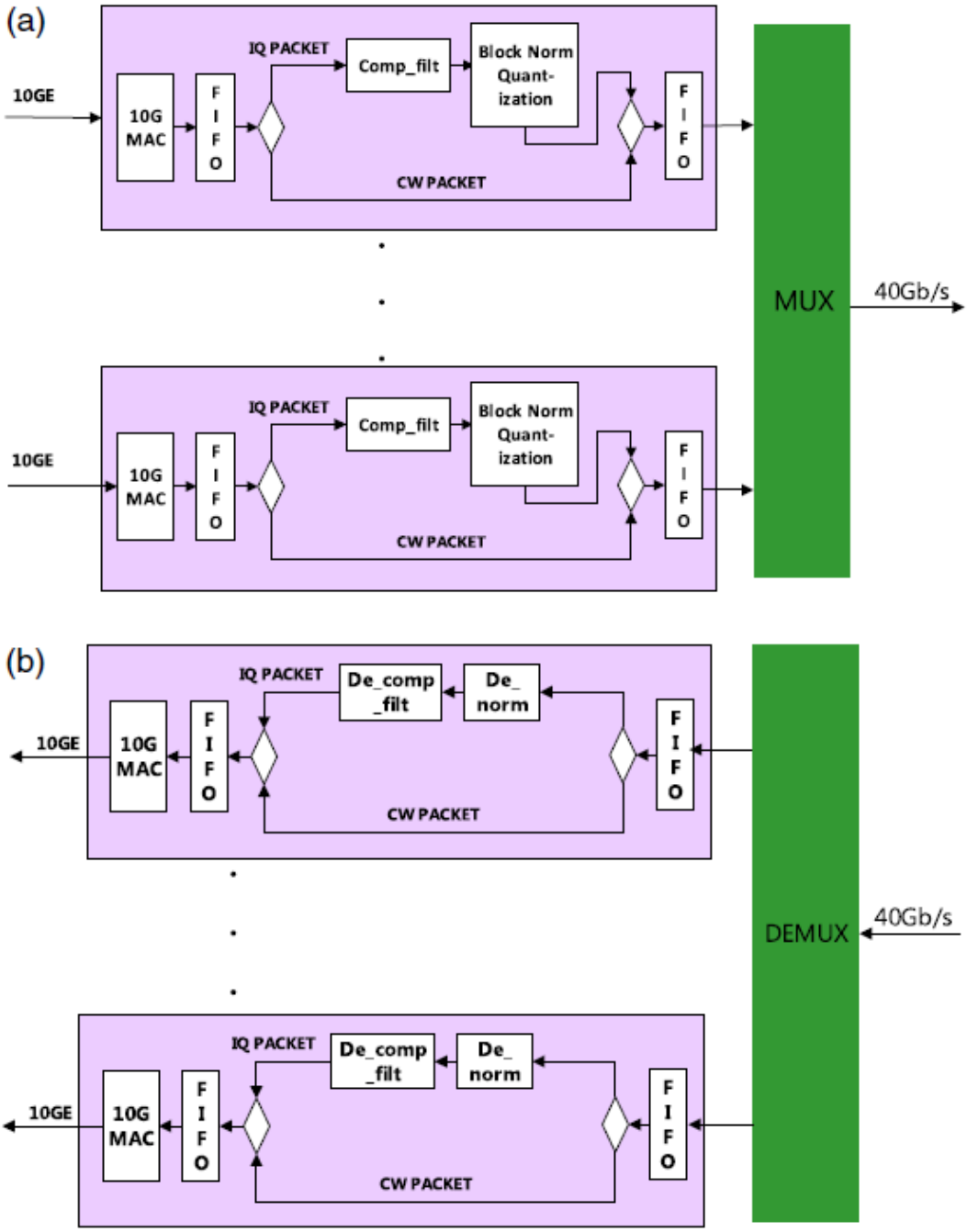

Figure 17. (a) Diagrammatic sketch in DSP transmitter; (b) Diagrammatic sketch in DSP receiver.[50]

Fig18 presents the outcomes of experiment. Obviously, restored radio frequency (RF) spectra conditions are good. Meanwhile, recovered Long-Term Evolution (LTE) signal has an error vector magnitude (EVM) of less than one percent. It has been enough to backup the 5G signal format, for

example 256-QAM.

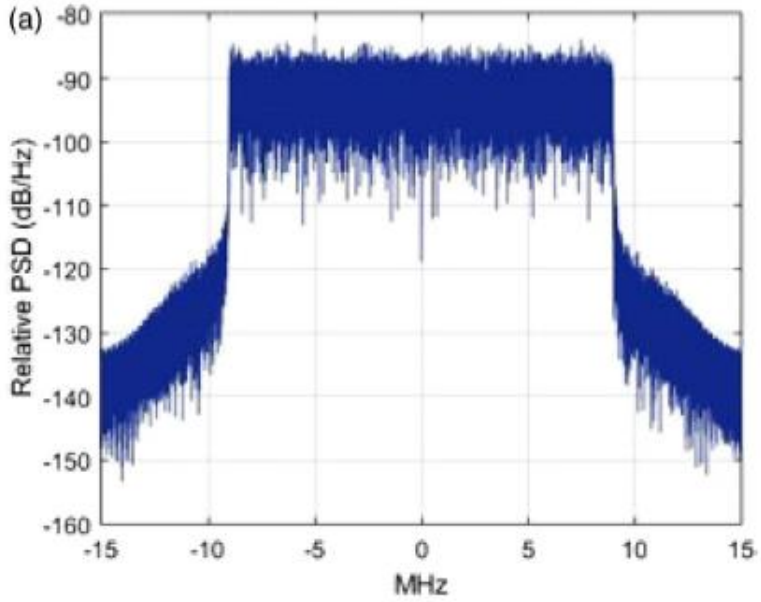

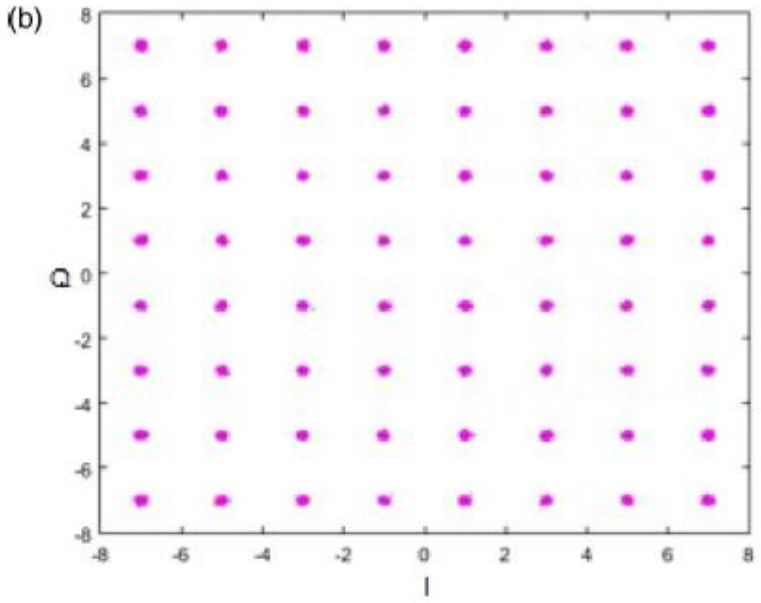

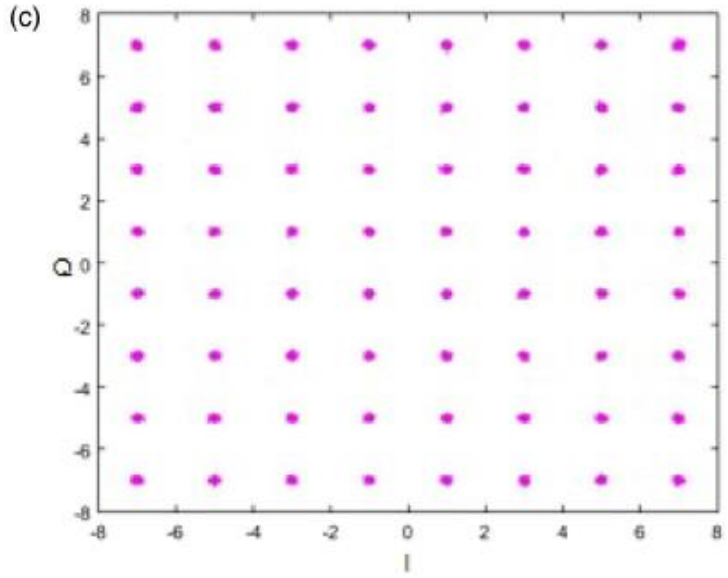

Figure 18. (a) Restored RF spectra in experiment, (b) restored signal constellation with no fiber transferring (L=zero kilometer), and (c) restored signal constellation when 10 kilometers transferring has been done (L=ten kilometers) to 1 particular 20 MHz LTE signal.[50]

Additionally, both low processing latency and high throughput is required in mobile fronthaul. The end to end delay typically recommended for 5G radio networks has been one ms, while delay assigned towards the fronthaul has been approximately two hundred μs. It has corresponded to back and forth trip latency delay resulting from the twenty kilometers SSMF connection. By thinking about fronthaul' covering range will be as long as twenty kilometers, the process of delay requires the small part of fiber circulation latency, such as <twenty μs. Back and forth delay process in actual-time CPRI system has been taken measurement as <twenty μs. The system of CPRI can as well interoperate with real baseband unit (BBU) as well as remote radio unit (RRU) devices without causing an obvious degrease within radio signal performance.

5.2 Low-Latency eCPRI-PON

The PON get the PTMP structure that will be particularly suitable for bringing eCPRI flow for sharing general fiber basic facilities through several RRU positions to achieve statistical multiplexing gain and reduce fiber cost, as shown in Figure 19. Time Division Multiplexing (TDM)-PON is very efficient, and should integrate eCPRI packs in the upstream into burst of TDM-PON, because every burst pays for overhead with synchronism as well as channel tracing aims. Fig 20 shows the distribution of uplink signal burst within a small delay eCPRI-PON in which the length of time of a TDM-PON period (T_{cycle}) is set when an Optical Line Terminal (OLT) reads Optical Network Unit (ONU). It will be basically equal to the symbol period (T_{sym}) of the wireless signal, for example ~50μs. Every ONU transmits all eCPRI packets in the manner of burst-by-burst by the burst time T_{burst}. Assigning every ONU the provided number of bursts of each period (NB) is able to achieve adaptable bandwidth assignment. An available gap circle T_{gap} will be assigned among neighboring bursts for avoiding burst collisions in actual systems. Therefore, Tcycle can also be expressed as $T_{cycle}=(T_{burst}+T_{gap})\cdot\Sigma^{N}_{i=1}\cdot NBi$, in which N has been the total ONU number within PON, while NBi has been burst each period per cycle allocated on the ith ONU.

For carrying eCPRI packs through the TDM-PON along with small delay, we suggest transferring every TDM-PON burst immediately when

aggregating several eCPRI packs in the upstream to the bursts, see Figure 21. It's achieved after coordinating RAN-MAC as well as PON-MAC.

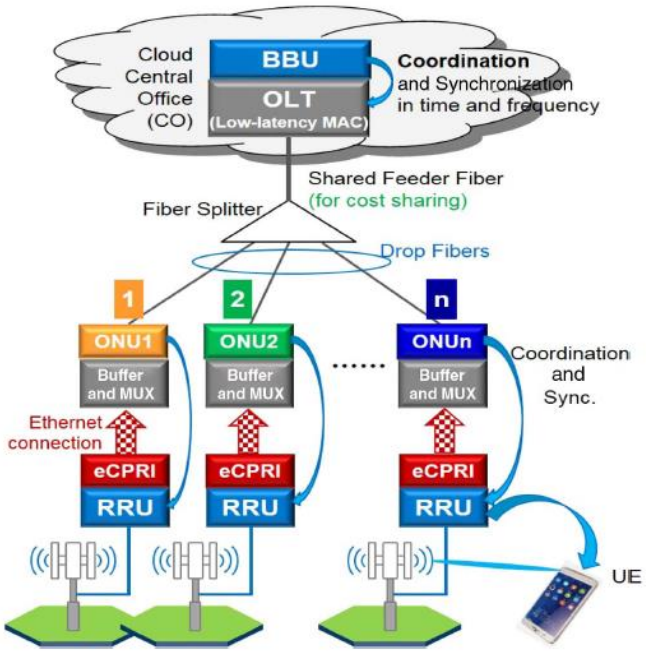

Figure 19. Figure for eCPRI-PON structure with low-latency.[15]

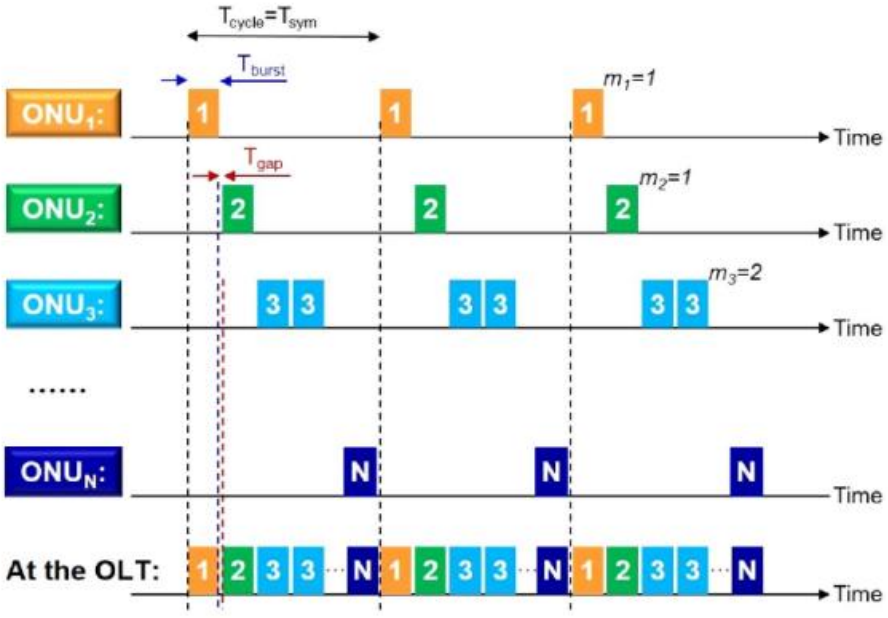

Figure 20. Illustration of upstream signal burst arrangement in the low-latency eCPRI-PON.[15]

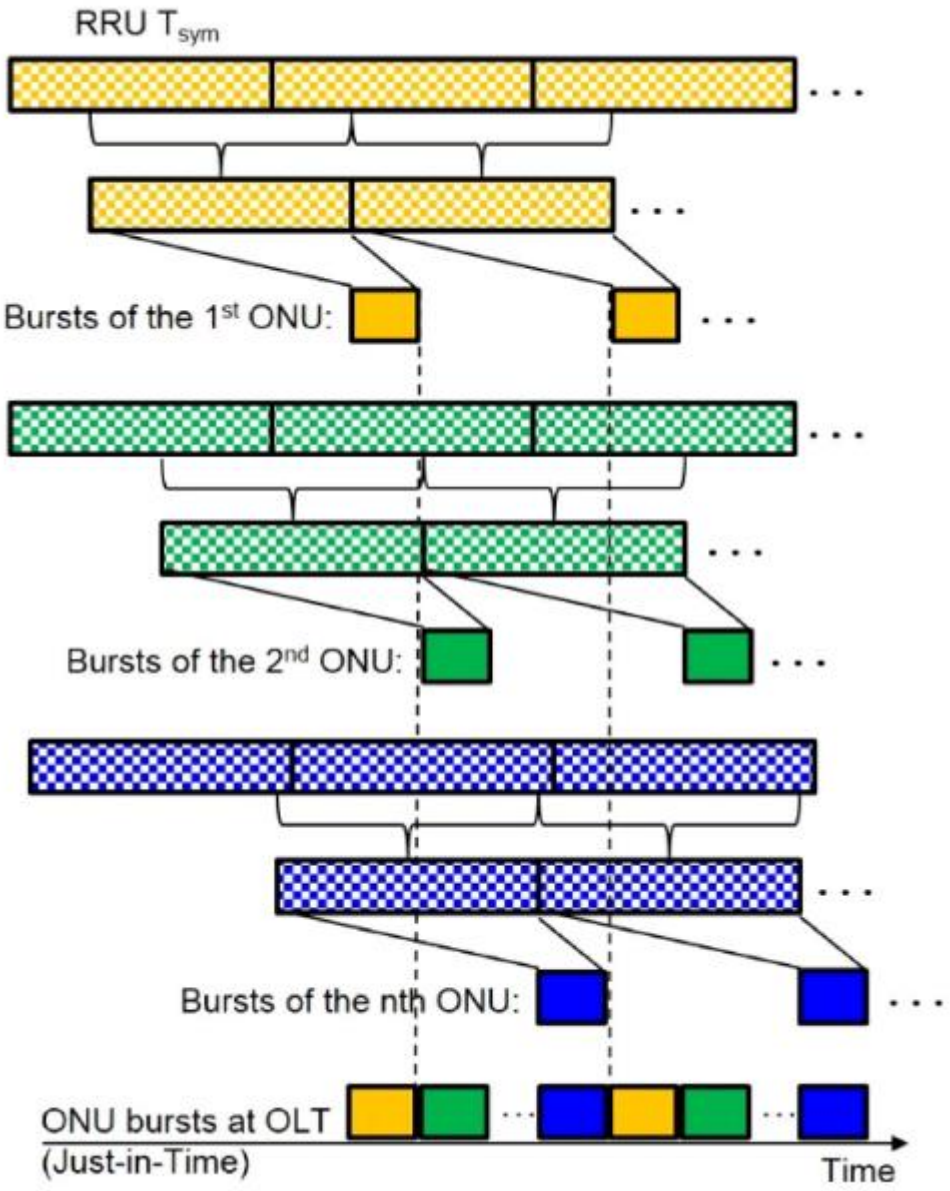

Figure 21. Figure for just-in-time integration of eCPRI packs to TDM-PON burst within eCPRI-PON with low-latency.[15]

Figure 22 shows the eCPRI-PON construction in the asymmetrical downstream and upstream. Now, frame title in the downstream is the codewords or 1984-bits, enough for containing required ONU data. Transferring effectiveness in the downstream will be $216/248\times(1000-1)\times1000=87\%$.

As in [15], a symmetric upstream and downstream eCPRI-PON

construction within an FPGA-based actual-time background is implemented. Fig 23 presents construction picture. Real delay process related to aggregation and FEC encoding of eCPRI packets is only about 45μs. It has been believed acceptable on 5G application with low-latency in which end-to-end delay is limited within 1 ms.

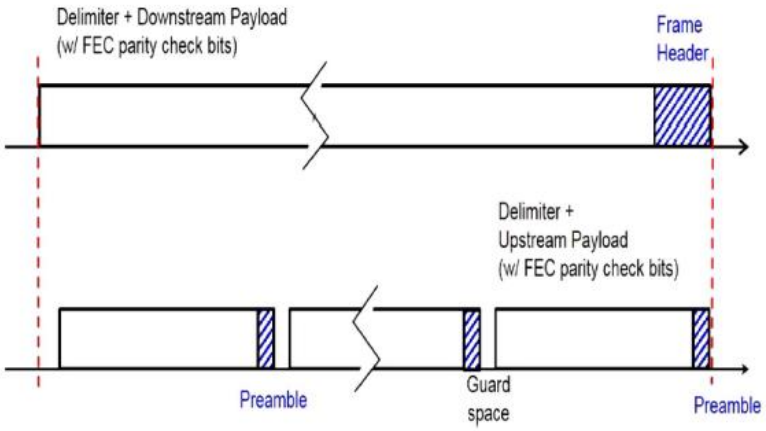

Figure 22. Illustration of an asymmetric downstream and upstream eCPRI-PON frame structure.[15]

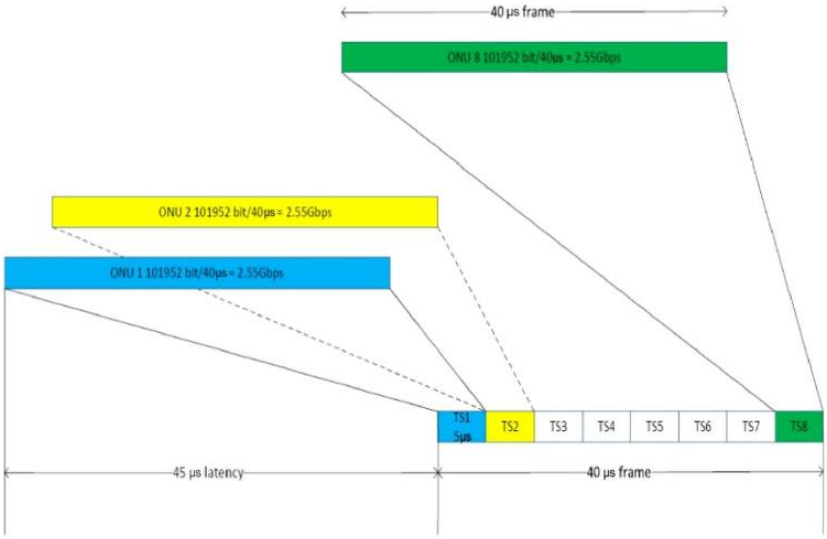

Figure 23. Illustration of an implemented symmetric downstream and upstream eCPRI-PON frame structure.[15]

Chapter 6 Time Controlled Haptic Optical Access

To satisfy the latency and bandwidth demand of 5G mobile services as well as the residential/enterprise services in following generation, we propose that it is the Time Controlled Haptic Optical Access (TIC-TOC) technology that implements the passive optical networks (PONs) with high-speed and low-latency. With adopting channel bonding as well as dynamic bandwidth allocation (DBA), TIC-TOC technology offers 5G mobile networks for low latency with the services of bandwidth-intensive and low-latency. Later, we will discuss this technic experimentally.

6.1 PON with High-speed as well as low-latency

Technology of TIC-TOC adopts channel binding with pack level and loop-based DBA over multiple wavelengths for supporting data rates, which may reach 100 Gb per second as well as delaying no more than 1 minute. Every wavelength operates with a data rate of 25 Gb/s and the total capacity of the four wavelengths can be extended to 100 Gb/s. Different from NG-PON2, every ONU can accept many wavelengths. Channel binding lets each single wavelength be transmitted at a limited data rate. Therefore, multi-speed ONUs will exist together within every ODN by channel binding.

Figure 24 indicates that it’s probable that ONU with multi-speed

coexists within a PON. PON is applied to the same ODN to mobile backhaul/fronthaul, as well as services of business and conventional residential [24],[51]. To adapt to 5G mobile services, especially depending on the QoS of the service type, it is necessary to guarantee high-bandwidth as well as low-delay of no more than one millisecond. A low-delay link with mobile services can be realized by a DBA with loop-base, whose cycle time is 250 μs. Generally, latency within conventional PON is mostly greater than a few milliseconds due to the use of poll-based bandwidth allocation.

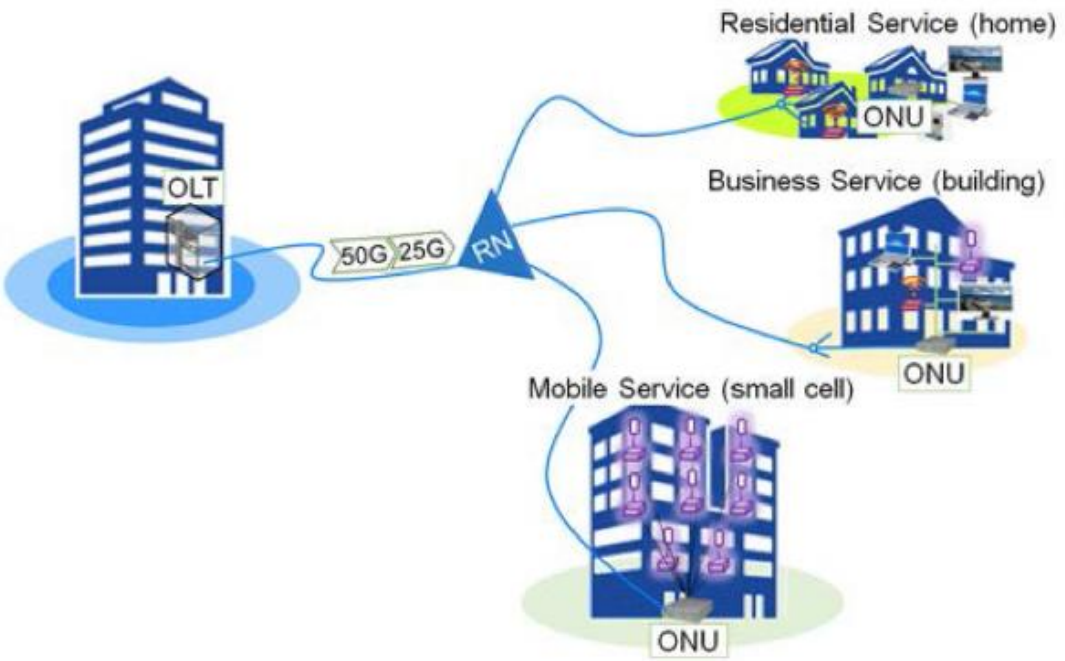

Figure 24. PONs with large-volume and low-latency in the future can accommodate the services of mobile, enterprise as well as residential within each ODN.[18]

6.1.1 DBA with Low latency

The bandwidth assignment methods within PON are generally classified to static bandwidth assignment (SBA) as well as dynamic bandwidth assignment (DBA). The bandwidth within the SBA will be assigned with normal time spans, while bandwidth assignment within the DBA varies depending on the state of the queue. Low latency is able to be provided by SBA, with low use of bandwidth, and with little latency performance bandwidth use of DBA is in a good condition. Therefore, the balance of SBA and DBA shows up.

Some efficient DBA algorithms can cut down latency within PON and use bandwidth. The DBA algorithm online which is dedicated to improve network utilization and inter-ONU fairness is on the basis of interleaved polling with adaptable circle period. The fast class-of-service oriented packet scheduling (FCOPS) for credit polling technology is proposed to provide end users with high network utilization and differential services. A fast class-of-service oriented packet scheduling (FCOPS) for technology of credit polling is put forward for providingend users with good network use as well as differentiated service. In upstream transmission in the previous DBA, the latency is about several milliseconds. In order to adapt the 5G mobile services through PON, it is necessary to guarantee bandwidth and low latency of no more than one minute. For meeting the the demand, we have presented a low latency oriented pack scheduling

(LOPS) on the basis of DBA are proposed by us. As various supports, within every ONU, we divide the class queues into gold, silver, bronze, as well as best effort (BE). Depending on quality of service (QoS) requirement, the incoming data packets can be divided into corresponding class queues, for instance the gold for leased line, expedited forwarded (EF) silver, as well as assured forwarded (AF) bronze. Services with low latency are divided as gold classed. Within LOPS, bandwidth in the upstream has first been assigned into gold class upstream using a scheme based on a static cycle. Later, the rest ones are dynamically assigned towards another category using weighted fair queuing (WFQ) based on credit which is the same to FCOPS. We guarantee latency together with bandwidth within gold class because at least once, the bandwidth is assigned to this class within no more than two cycles in the LOPS. Thus, it is possible to have low-latency within gold class to 5G mobile traffic as well as using bandwidth efficiently for business and residential services.

6.2 Experiment setup

Figure 25(a) is an experimental setup done by [18] for presentation for PON with high-speed and low-latency to 5G wireless network. Prototype has been called TIC-TOC because it can guarantee bandwidth together with low-latency for 5G wireless network. In this hypothetical scenario, ONU1 has been applied to 5G mobile backhaul, while ONU2 is used for operating business or residential services as well as ONU3. ONU1 adopts 2 WDM channels for providing downstream capacity of 50 Gb/s and upstream capacity of 20 Gb/s, while ONU3 use just a single WDM channel and has capacity with 25 Gb/s and 10 Gb/s. ONU and OLT are set up of PON MAC within FPGA, transceivers of PON as well as several 10 Gb/s Ethernet (10GbE) ports. PON MAC is composed with LOPS-based DBA, QoS, OAM, MPCP as well as channel boding functions in order to manage several ONUs with operating signals in downstream at a rate of 2 x 25 Gb/s together with 2 × 10 Gb/s in upstream. As within Figure 25(b), on the basis of avalanche photo-diode (APD) as well as receiver optical subassembly (ROSA), transceivers of PON OLT and ONU that can be plugged in are implemented. The transceivers are use to accommodate 2x25 Gb/s signals within downstream and 2x10 Gb/s signals within upstream. These signals are in ODN with SMF of twenty kilometers and 64-split cost efficiency. The modulation is non-return to zero (NRZ) for both downstream and upstream. And we use the little factor pluggable pack for presenting the

pluggable PON transceiver.

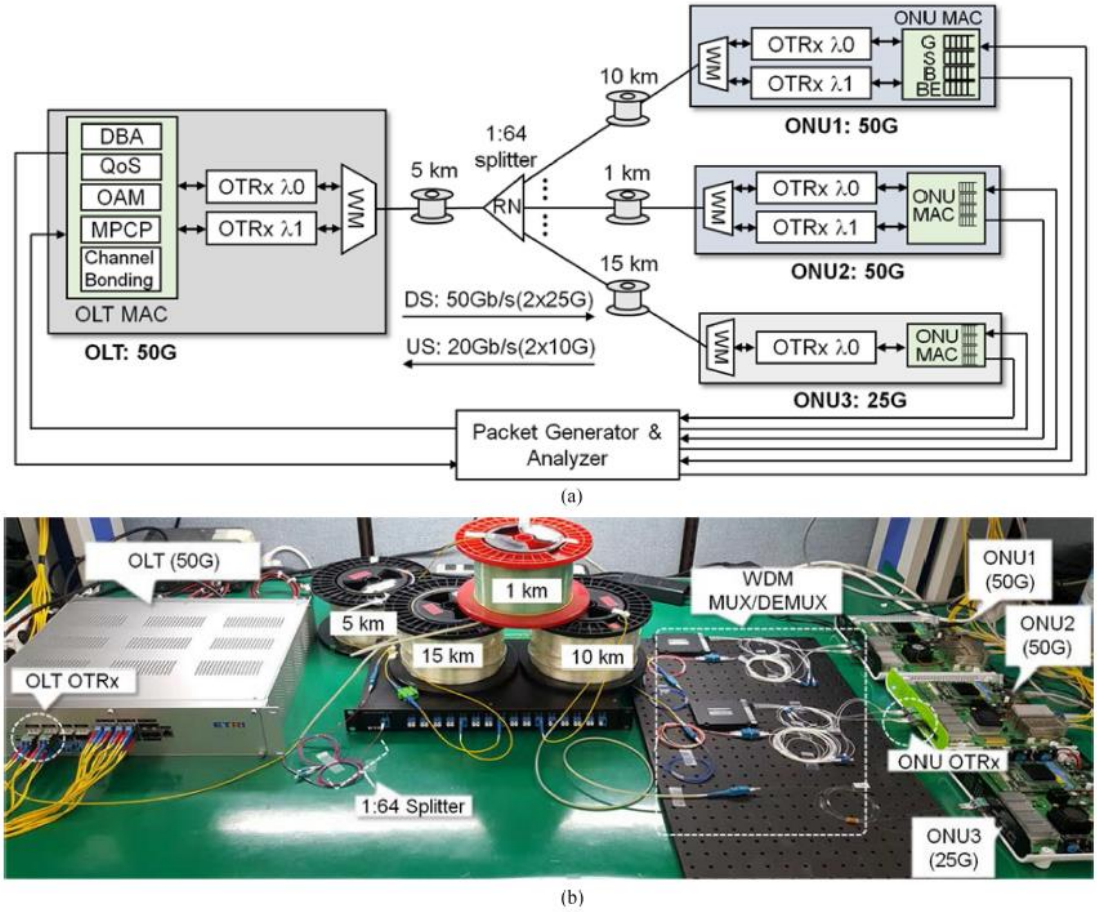

Figure 25. Experiment setup on demonstrating PON with high speed and low latency for 5G wireless networks (a) connect 50 Gb / s OLT, 25 Gb / s ONU as well as two 50 Gb / s ONU with link configurations, (b) finished diagram of the test bench.[18]

6.3 Results and discussion

6.3.1 Link performance

In the Physical Medium Dependent (PMD) layer of a TIC-TOC system with a 25 Gb / s signal in the downstream as well as a 10 Gb / s signal in the upstream, the function of bit error rate (BER) has been measured. The solid fill symbol in Figure 26(a) shows the measured back-to-back BER performance of the signals in the upstream and downstream with an ER of 8 dB as well as a 2^{31}-1 length PRBS. The hollow unfilled symbol indicates the measured BER performance after transmitting twenty kilometers of signals in downstream as well as upstream. When transmitting more than twenty kilometers the electricity loss is negligible of the cases because of the dispersion tolerance within the O-band transferring. The inset within Figure 26(a) is the optical eye figure measured back-to-back when transmitting more than twenty kilometers. There are no obvious different points among eye figures. We must use a forward error correction (FEC) in PCS layer since the output power of OLT transmitter is limited. We use FEC to achieve the 10^{-12} BER when transmitting a complete ODN (twenty kilometers SMF, 64 separator and WM). By using FEC, we are unable to get the wrong pack transmission. Figure 26(b) indicates a measurement of optical waveform for BM 10Gb/s signal in the upstream. We're sure that 10 ns after turning on the laser, the output power of the laser becomes stable.

Then start to transmit the preamble pattern. Thus, there's possibility to decrease the time of upstream packet of BM overhead.

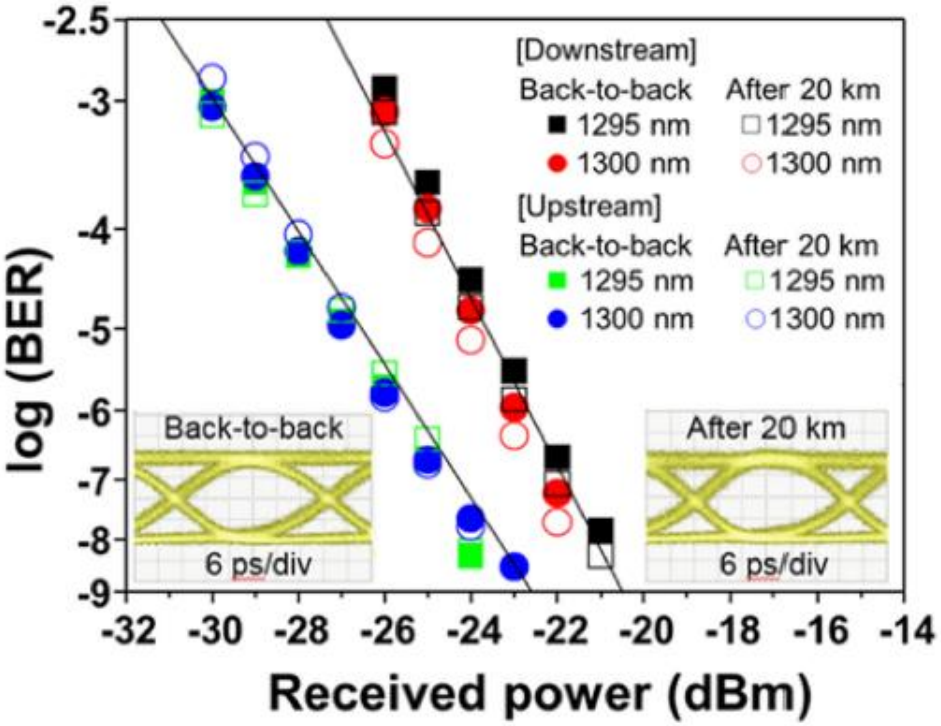

(a)

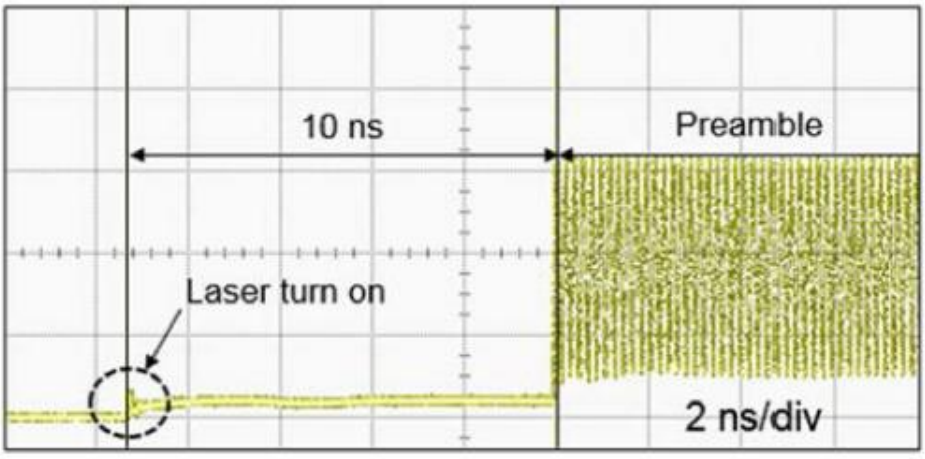

(b)

Figure 26. The BER and eye figures (a) performance of 2 × 25gb / s downlink as well as 2 × 10Gb / s uplink are measured. (b) upstream signal waveform of pulse mode, the starting time of laser is 10ns.[18]

6.3.2 Low latency operation

We do an evaluation of the latency in real-time traffic. The measurement of the latency is the packs' round-trip period back to pack generators and parsers. The second table indicates the condition of input traffic of the three ONUs. As we can see, ONU1 has been only set within the gold queuing, while ONU2 and ONU3 have be set within silver, bronze as well as BE queuing. Round trip time setting will be 250μs and the total bandwidth in uplink will be 16 Gb/s. The capacity of every class line takes 8 MB within the ONU. The load provided toward ONU1 will be set to be a 6 Gb / s constant rate, and the load provided to ONU2 as well as ONU3 will be changed 1 Gb / s into 10 Gb / s. Input packs towards ONU2 as well as ONU3 have been sorted into 3 category lines with the right rate. In order to measure the max latency, we use the packets with 1518 bytes. Generally, since the packets within ONU are dealt with the method of save and forward, the latency increases when we use longer packets. Therefore, we used the largest length of Ethernet packets. For the priority policy, the weights for silver, bronze, as well as BE within the WFQ algorithm have been set as 2:1:1. 6.2 Gb / s static bandwidth will be assigned into ONU1. In the case of that the load for ONU2 as well as ONU3 goes up by 1 Gb/s in order, we measure the delay.

ONU	Total Offered Load (Gb/s)	Uplink BW (Gb/s)	Offered Service			Weight
			Type	Service Ratios (%)	Mode	
ONU1 (50G)	6	Total 16	Gold	100	Static	-
ONU2 (50G)	1 ~ 10		Silver	33	Dynamic	2
			Bronze	33		1
			BE	33		1
ONU3 (25G)			Silver	33		2
			Bronze	33		1
			BE	33		1

Table 2. Input traffic condition to verify the LOPS algorithm.

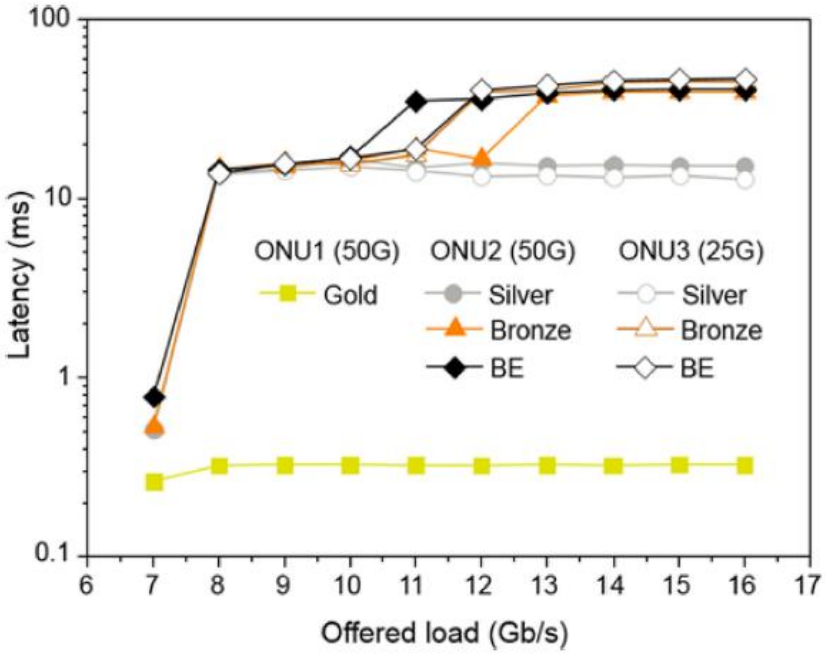

Figure 27. Measured latency in gold, silver, bronze, and best effort class as a function of offered load.[18]

Figure 27 is the result of the latency that is measured. The vertical axis is the latency that is measured while the horizontal axis is the provided load to all of ONUs. In the gold class, the latency is always less than 400μs even the traffic load becomes larger. As the number of the gold traffic increases, the allocation time of the traffic transmission will increase, which decrease the latency. In other words, the latency increases if the gold traffic is less. Thus, if the gold traffic is very few, the latency will reach to maximum. By

using equation (1), we can compute the latency of ONU1, which is about 481µs where F_{delay} is about 75µs (15km). obviously, the latency measured is better than the computed one. If in the worst case we can connect more ONUs, the latency will be closer to the delay that is computed. Because of the priority, the silver class latency is stable at the traffic load of over 8 Gb/s, whereas the latency of bronze and the BE becomes larger because of the packet loss.

$$\begin{aligned} latency\_h_{\max} &= qt\_h_{max} + F_{delay} \\ &= 2 \times T_{cycle} - T_{alloc} + F_{delay} \end{aligned}$$

Equation (1).

Chapter 7 Conclusion

No matter which architecture we are using, current 5G networks already have strict requirements on transport networks, in terms of both capacity and latency. We have reviewed the mature optical transport technics which can satisfy the current specifications. However, in practical, we still need to pay a lot of efforts to transfer the industry solutions to commercial products. We have presented some simulations of network architecture such as VCRAN to show that comparing to the traditional RAN, VCRAN has higher throughput and is more energy efficient. We presented the potential of a QPAR device in 5G backhaul networks. The QPAR node in a shared hierarchical packet-switched network (e.g., PON) reduces the latency under unbalanced loads and the PPAR node can be remotely powered due to the low steady-state power consumption. DSP was also reviewed which can enable fast burst-mode signal recovery to achieve low-latency operation in PTMP architectures such as CPRI/eCPRI over TDM-PON. At last, we discussed the high-speed and low latency PON enabled by time controlled-tactile optical access technology supporting channel bonding and low-latency DBA for the accommodation in 5G mobile, business, and residential services. All the results confirmed that the multiwavelength PON could support bandwidth-intensive as well as low-latency services for 5G mobile network. There’re a lot of technics which can reduce the latency while guarantee bandwidth and QoS, we believe in

the future we can bring a more complete and practical solution using in 5G networks.

Acknowledgement

I really appreciate Professor CURRI VITTORIO and Doctor FERRARI ALESSIO for the support and advice of my thesis. I also would like to appreciate all my friends and family for all the support during my master degree.

Reference

[1] “Transport Evolution for the RAN of the Future [Invited],” VOL. 11, NO. 4/APRIL 2019/J. OPT. COMMUN. NETW. B97.

[2] xRAN, “Next generation RAN architecture,” 2018 [Online]. Available: https://www.xran.org.

[3] xRAN, “xRAN forum merges with C-RAN Alliance to form ORAN Alliance,” Feb. 2018 [Online]. Available: https://www .o-ran.org/news/.

[4] “Joint Allocation of Radio and Optical Resources in Virtualized Cloud RAN with CoMP,” Xinbo Wang, Cicek Cavdar, Lin Wang, Massimo Tornatore, Yongli Zhao, Hwan Seok Chung, Han Hyub Lee, Soomyung Park, and Biswanath Mukherjee University of California Davis, USA; KTH Royal Institute of Technology, Sweden; Politecnico di Milano, Italy; Beijing University of Posts and Telecommunication, China Electronics and Telecommunications Research Institute, Korea.

[5] Cisco, ‘‘Visual Networking Index: Forecast and Methodology, 2014---2019,’’ May. 2015.

[6] Next generation mobile network alliance, “RAN Evolution project CoMP evaluation and enhancement,” Mar. 2015.

[7] China Mobile Research Institute, “C-RAN: The road towards green RAN V3.0,” Dec. 2013.

[8] T. Pfeiffer, “Next Generation Mobile Fronthaul and Midhaul

Architectures," Journal of Optical Communications and Networking, vol. 7, no. 11, pp. B38-B45, Nov. 2015.

[9] ‘‘Further advancements for E-UTRA physical layer aspects v.9.0.0,’’ 3GPP TR 36.814, 2010.

[10] "Quasi-Passive Optical Infrastructure for Future 5G Wireless Networks: Pros and Cons," VOL. 8, NO. 12/DECEMBER 2016/J. OPT. COMMUN. NETW. B111.

[11] T. Pfeiffer, "Next generation mobile fronthaul and midhaul architectures [Invited]," J. Opt. Commun. Netw., vol. 7, no. 11, pp. B38–B45, 2015.

[12] 5G PPP Architecture Working Group, "View on 5G architecture," July 2016 [Online]. Available: https://5g-ppp.eu/ wp-content/uploads/2014/02/5G-PPP-5G-Architecture-WP-Forpubli c-consultation. pdf.

[13] Y. Bi, J. Jin, and L. G. Kazovsky, "Quasi-passive reconfigurable optical node: First experimental demonstration," in Conf. on Lasers and Electro-Optics (CLEO), 2012, paper CTh1H.5.

[14] Y. Bi, S. Shen, J. Jin, K.Wang, and L. G. Kazovsky, "Remotely powered and reconfigured quasi-passive reconfigurable nodes for optical access networks," J. Electr. Comput. Eng., vol. 2016, 2938415, 2016.

[15] "Digital Signal Processing for High -Speed Fiber-Wireless

Convergence [Invited],” VOL. 11, NO. 1/JANUARY 2019/J. OPT. COMMUN. NETW. A11

[16] “Common Public Radio Interface (CPRI): Interface Specification,” CPRI Specification V7, Oct. 2015.

[17] X. Liu, H. Zeng, N. Chand, and F. Effenberger, “Efficient mobile fronthaul via DSP-based channel aggregation,”
J. Lightwave Technol., vol. 34, no. 6, pp. 1556–1564, Mar. 2016.

[18] “High Speed and Low Latency Passive Optical Network for 5G Wireless Systems,” JOURNAL OF LIGHTWAVE TECHNOLOGY, VOL. 37, NO. 12, JUNE 15, 2019.

[19] IEEE 5G, IEEE 5G and Beyond Technology Roadmap White Paper, Oct. 2017. [Online]. Available: https://5g.ieee.org/roadmap.

[20] Ed Harstead, “25G based PON technology,” presented at the Opt. Fiber Commun. Conf., San Diego, CA, USA, Mar. 2018, doi: https://doi.org/10.1364/OFC.2018.Tu2B.5.

[21] X. Liu and F. Effenberger, “Emerging optical access network technologies for 5gwireless [Invited],” J. Opt. Commun. Netw., vol. 8, no. 12, pp. 70–79, Dec. 2016.

[22] Broadband Forum NG-PON2 Project, the first PON standard optimized for service convergence, 2018. [Online]. Available: https://www.broadband-forum.org/ng-pon2.

[23] L. Zhang, Y. Luo, B. Gao, X. Liu, F. Effenberger, and N. Ansari,

"Channel bonding design for 100Gb/s PON based on fec codeword alignment," presented at the Opt. Fiber Commun. Conf., Los Angeles, CA,USA,Mar. 2017. doi: https://doi.org/10.1364/OFC.2017.Th2A.26.

[24] G. Kramer, B. Mukherjee, and G. Pesavento, "IPACT a dynamic protocol for an ethernet PON (EPON)," IEEE Commun. Mag., vol. 40, no. 2, pp. 74–80, Feb. 2002. doi: 10.1109/35.983911.

[25] T. Tashiro et al., "A novel DBA scheme for TDM-PON based mobile fronthaul," presented at the Opt. Fiber Commun. Conf., San Francisco, CA, USA, 2014. doi: 10.1364/OFC.2014.Tu3F.3.

[26] IEEE 802.3TM-2012, "IEEE Standard for Ethernet," 2012.

[27] 5G Alliance for Connected Industries and Automation (ACIA), "5G for connected industries and automation," Apr. 2018 [Online]. Available: https://www.5g-acia.org/publications/5g-forconnected-industries-and-automation-white-paper.

[28] Common Public Radio Interface, "CPRI/eCPRI specification," 2017 [Online]. Available: http://www.cpri.info/spec.html.

[29] "IEEE Standard for Local and Metropolitan Area Networks— Audio Video Bridging (AVB) Systems," IEEE Standard 802.1BA, 2011.

[30] "IEEE Standard for Local and Metropolitan Area Networks— Bridges and Bridged Networks—Amendment 26: Frame Preemption," IEEE Standard 802.1Qbu, 2016.

[31] N. J. Gomes, P. Sehier, H. Thomas, P. Chanclou, B. Li, D. Münch, P.

Assimakopoulos, S. Dixit, and V. Jungnickel, “Boosting 5G through Ethernet,” IEEE Veh. Technol. Mag., vol. 13, no. 1, pp. 74–84, Mar. 2018.

[32] Microsemi, “Enabling C-RAN: The case for OTN mobile fronthaul,” White paper PMC-2143908, Nov. 2017 [Online]. Available: http://pmcs.com/cgi-bin/download_p.pl?res_id=277541.

[33] H. Li, L. Han, R. Duan, and G. M. Garner, “Analysis of the synchronization requirements of 5G and corresponding solutions,” IEEE Common. Stand. Mag., vol. 1, no. 1, pp. 52–58, 2017.

[34] T. Pfeiffer, “Next generation mobile fronthaul and midhaul architectures,” J. Opt. Commun. Netw., vol. 7, no. 11, pp. B38–B45, Nov. 2015.

[35] W. C. Cheung, et al., "Throughput Optimization, Spectrum Allocation, and Access Control in Two-Tier Femtocell Networks," IEEE J. on Selected Areas in Common., vol. 30, no. 3, pp. 561-574, Apr. 2012.

[36] A. Tanaka, et al., “Software Defined Flexible Optical Access Networks Enabling Throughput Optimization and OFDM-Based Dynamic Service Provisioning for Future Mobile Backhaul,” IEICE Transactions on Communications, vol. 97, no. 7, pp. 1244-1251, Jul. 2014.

[37] Y. Zhou and W. Yu, “Optimized backhaul compression for uplink cloud radio access network,” IEEE J. on Selected Areas in Commun.,

vol. 32, no. 6, pp. 1295-1307, June 2014.

[38] L. Zhou and W. Yu, “Uplink multicell processing with limited backhaul via per-base-station successive interference cancellation,” IEEE J. on Sel. Areas in Commun., vol. 30, no. 10, pp. 1981–1993, Oct. 2013.

[39] G. Nigam, et al., “Coordinated multipoint joint transmission in heterogeneous networks,” IEEE Transactions on Communications, vol. 62, no. 11, pp. 4134-4146, Nov. 2014.

[40] Next generation mobile network alliance, ‘‘Further Study on Critical CRAN Technologies,’’ Mar. 2015.

[41] A. Checko et al., ‘‘Cloud RAN for Mobile Networks----A Technology Overview," IEEE Communications Surveys & Tutorials, vol. 17, no. 1, pp. 405-426, 2015.

[42] D. Iida et al., "Dynamic TWDM-PON for Mobile Radio Access Networks," Optics Express, vol. 21, no. 22, pp. 26209-26218, 2013.

[43] ‘‘Further advancements for E-UTRA physical layer aspects v.9.0.0,’’ 3GPP TR 36.814, 2010.

[44] X. Wang et al., “Energy-Efficient Virtual Base Station Formation in Optical-Access-Enabled Cloud-RAN,” IEEE J. on Selected Areas in Commun., vol. 34, no. 6, Jan. 2016.

[45] Y. Bi, J. Jin, A. R. Dhaini, and L. G. Kazovsky, “QPAR: A quasi-passive reconfigurable green node for dynamic resource management

in optical access networks," J. Lightwave Technol., vol. 32, no. 6, pp. 1104–1115, 2014.

[46] Y. Bi, S. Shen, J. Jin, K.Wang, and L. G. Kazovsky, "Remotely powered and reconfigured quasi-passive reconfigurable nodes for optical access networks," J. Electr. Comput. Eng., vol. 2016, 2938415, 2016.

[47] T. A. Strasser and J. L. Wagener, "Wavelength-selective switches for ROADM applications," IEEE J. Sel. Top. Quantum Electron., vol. 16, no. 5, pp. 1150–1157, 2010.

[48] K. Wang, Y. Bi, and L. G. Kazovsky, "Bidirectional quasipassive reconfigurable (Bi-QPAR) node for flexible access networks," in Conf. on Lasers and Electro-Optics (CLEO), San Jose, CA, 2016, paper JTh2A.123.

[49] N. Shibata, T. Tashiro, S. Kuwano, N. Yuki, Y. Fukada, J. Terada, and A. Otaka, "Performance evaluation of mobile front-haul employing Ethernet-based TDM-PON with IQ data compression [Invited]," J. Opt. Commun. Netw., vol. 7, no. 11, pp. B16–B22, 2015.

[50] S. Megeed, X. Liu, H. Zeng, and F. Effenberger, "Demonstration of a FPGA-Based CPRI-over-ethernet real-time system achieving 120 Gb/s throughput over a 10-km SSMF link with 16 bi-directional 10GE connections," in Optical Fiber Communications Conf. and Exhibition (OFC), 2017, paper Th4B.2.

[51] H. H. Lee et al., “Real-time demonstration of QoS guaranteed 25-Gb/s PON prototype with Ethernet-PON MAC/PHY and cost-effective APD receivers for 100-Gb/s access networks,” Opt. Express, vol. 24, no. 13, 2016, Art. no. 13984.